

A Semi-Analytic Algorithm for Constructing Lower Dimensional Elliptic Tori in Planetary Systems. *

MARCO SANSOTTERA

Dipartimento di Matematica, Università degli Studi di Milano,
via Saldini 50, 20133 — Milano, Italy.

UGO LOCATELLI

Dipartimento di Matematica, Università degli Studi di Roma “Tor Vergata”,
Via della Ricerca Scientifica 1, 00133–Roma (Italy).

ANTONIO GIORGILLI

Dipartimento di Matematica, Università degli Studi di Milano,
via Saldini 50, 20133 — Milano, Italy.

e-mails: `marco.sansottera@gmail.com`, `locatell@mat.uniroma2.it`
`antonio.giorgilli@unimi.it`

Abstract

We adapt the Kolmogorov’s normalization algorithm (which is the key element of the original proof scheme of the KAM theorem) to the construction of a suitable normal form related to an invariant elliptic torus. As a byproduct, our procedure can also provide some analytic expansions of the motions on elliptic tori. By extensively using algebraic manipulations on a computer, we explicitly apply our method to a planar four-body model not too different with respect to the real Sun–Jupiter–Saturn–Uranus system. The frequency analysis method allows us to check that our location of the initial conditions on an invariant elliptic torus is really accurate.

1 Introduction

Since the birth of KAM theory (see [22], [39] and [1]), invariant tori are expected to be the key dynamical objects which may explain the (nearly perfect) quasi-periodicity

**Key words and phrases:* KAM theory, lower dimensional invariant tori, normal form methods, n-body planetary problem, Hamiltonian systems, Celestial Mechanics. *2010 Mathematics Subject Classification.* Primary: 37J40; Secondary: 37N05, 70F10, 70–08, 70H08.

of the planetary motions of our Solar System. On the other hand, Poincaré has widely discussed the role of periodic orbits, namely of one-dimensional tori. A natural extension is the search for lower dimensional invariant tori, which are characterized by quasi-periodic motions with a number of frequencies lower than the actual number of degrees of freedom of the system.

In the case of a planetary system including n planets it seems natural to look for particular orbits, namely solutions of Newton's equations lying on n -dimensional tori, the latter being slight deformations of the composition of n *coplanar circular* Keplerian orbits. This in view of Lagrange theory of secular motions, where, in the frame of the so-called *secular model*, circular orbits are considered as a first approximation and the motions of eccentricities and inclinations are represented as small oscillations with respect to the reference orbit. Replacing the circular orbit with an elliptic lower dimensional torus, i.e., a torus which is stable with respect to small oscillations around it, we expect to find a better starting point for a secular theory.

The aim of this paper is to present an explicit algorithm, based on the original Kolmogorov's one, for constructing elliptic tori for a model including three of the biggest planets. We also perform an explicit calculation via algebraic manipulations and a comparison of the orbits so found with the outcome of a numerical integration of Newton's equations.

It should be emphasized that the existence of elliptic lower dimensional invariant tori is not a straightforward consequence of Kolmogorov's theorem.

The existence of lower dimensional tori in the planetary problem (both elliptic or hyperbolic) has been proven by Jefferys and Moser (see [18]) and Lieberman (see [34]). A general theorem has been proved by Pöschel (see [43] and [44]). An application of Pöschel's method to the Solar System has been produced by Biasco, Chierchia and Valdinoci in two different cases, namely the spatial three-body planetary problem and a planar system with a central star and n planets (see [4] and [5], respectively). However, as it often happens in the framework of KAM theory, their approach is a deep one from a theoretical point of view, but seems not to be suitable for explicit calculations, even if one is interested just in finding the locations of the elliptic invariant tori. Let us clarify this point.

The results of Biasco, Chierchia and Valdinoci are based on performing a sequence of canonical transformations that give the Hamiltonian a particular form to which Pöschel's theorem can be applied. In turn, Pöschel's theorem is based on a clever adaptation of Arnold's proof of KAM theorem. Precisely, the perturbation is removed by a sequence of canonical transformations which are defined on a subset of the phase space excluding the "resonant regions" (see [1] and [2]). The procedure ends up with a nowhere dense Cantor set of elliptic invariant tori. Although effective from the analytical viewpoint, the procedure looks hardly applicable in a practical calculation.

The original scheme of the proof introduced by Kolmogorov is in a much better position for what concerns the translation into an explicit algorithm (see [22], [3], [13] and [14]). Such an approach has been successfully used to calculate the orbits for some interesting problems in Celestial Mechanics (see [35], [36], [37] and [11]). Thus, we think it is useful to modify Kolmogorov's algorithm so as to be able to construct a suitable normal form related to the elliptic tori. In addition, this will allow us to explicitly integrate the equations of

motion on those invariant surfaces, by using a so-called semi-analytic procedure.

An explicit construction of elliptic (or maybe hyperbolic) lower dimensional tori may be useful in many cases. We pay some attention to (a) the problem of the long term stability of orbits in the planetary system, and (b) the possible application to the search for orbits suitable for spatial missions.

Concerning the long term stability of a planetary system, the construction of a normal form related to some fixed elliptic torus could be a relevant milestone. It is indeed possible to ensure the effective stability in the neighborhood of such an invariant surface by implementing a partial construction of the Birkhoff normal form. A similar approach in the neighborhood of either a maximal dimensional KAM torus or of the circular orbits has been worked out, e.g., in [20], [15] and [16]. Concerning our Solar System, such an approach might be applied to some asteroids with small orbital eccentricities and inclinations. However, as explained in [46], this same approach can not yet succeed in proving the long-time stability of the major planets of our Solar System.

Concerning spatial missions, the strong stability of the regions close to elliptic invariant tori may be very useful in identifying stable orbits. Moreover, our technique should also adapt quite easily to the construction of hyperbolic tori that can be used in the design of spacecraft missions requiring low energy transfers. We also recall that lower dimensional tori of elliptic, hyperbolic and mixed type have been studied in the vicinity of the Lagrangian points for both the restricted three-body problem and the bicircular restricted four-body problem (see, e.g., [19], [21], [8] and [10]).

The paper is devoted to the construction of elliptic tori for a model not far from the Sun–Jupiter–Saturn–Uranus (SJSU) *planar* system (let us recall that the real orbits of the planets of our Solar System *are presumably not* lying on lower dimensional tori). By the way, we think that with some minor modifications our procedure should adapt also to the more general spatial case, after having performed the reduction of the angular momentum, which is not considered here in order to shorten the description of all the preliminary expansions (for an introduction to some methods performing both the partial and the total reduction, see [9], [38] and [40]). The contents are organized as follows.

Sect. 2 is devoted to the introduction of our Hamiltonian model and to a schematic description of its expansion in canonical coordinates. This will allow us to write down the form of the Hamiltonian to which our approach can be applied.

Our algorithm constructing a normal form for elliptic tori is presented in a purely formal way in sect. 3. In subsect. 3.4 we briefly introduce the theoretical background necessary to investigate the convergence. We plan to give all details about convergence in a future work (see [17]).

Sect. 4 is devoted to an application which we also use as a test of our procedure. First, in subsects. 4.1–4.2 we describe the implementation of our algorithm, by using an algebraic manipulator on a computer so to produce both the normal form and the semi-analytic integration of the motion on an invariant elliptic torus. Then in sect. 4.3 we check the accuracy of our construction by using frequency analysis. This is based on the fact that the Fourier spectrum of the motions on elliptic tori is strongly characteristic, because only the mean-motion frequencies and their linear combinations can show up.

2 Classical Expansion of the Planar Planetary Hamiltonian

We apply our algorithm for constructing elliptic tori to a concrete planetary model. We consider four point bodies P_0, P_1, P_2, P_3 , with masses m_0, m_1, m_2, m_3 , mutually interacting according to Newton's gravitational law. Hereafter we associate the indexes 0, 1, 2, 3 to Sun, Jupiter, Saturn and Uranus, respectively.¹

Let us now recall how the classical Poincaré's variables can be introduced so to perform a first expansion of the Hamiltonian around circular orbits, i.e., having zero eccentricity. We basically follow the formalism introduced by Poincaré (see [41] and [42]; for a modern exposition, see, e.g., [29] and [30]). We remove the motion of the center of mass by using heliocentric coordinates $\mathbf{r}_j = \overrightarrow{P_0 P_j}$, with $j = 1, 2, 3$. Denoting by $\tilde{\mathbf{r}}_j$ the momenta conjugated to \mathbf{r}_j , the Hamiltonian of the system has 6 degrees of freedom, and reads

$$F(\tilde{\mathbf{r}}, \mathbf{r}) = T^{(0)}(\tilde{\mathbf{r}}) + U^{(0)}(\mathbf{r}) + T^{(1)}(\tilde{\mathbf{r}}) + U^{(1)}(\mathbf{r}), \quad (1)$$

where

$$\begin{aligned} T^{(0)}(\tilde{\mathbf{r}}) &= \frac{1}{2} \sum_{j=1}^3 \frac{m_0 + m_j}{m_0 m_j} \|\tilde{\mathbf{r}}_j\|^2, & T^{(1)}(\tilde{\mathbf{r}}) &= \frac{1}{m_0} \left(\tilde{\mathbf{r}}_1 \cdot \tilde{\mathbf{r}}_2 + \tilde{\mathbf{r}}_1 \cdot \tilde{\mathbf{r}}_3 + \tilde{\mathbf{r}}_2 \cdot \tilde{\mathbf{r}}_3 \right), \\ U^{(0)}(\mathbf{r}) &= -\mathcal{G} \sum_{j=1}^3 \frac{m_0 m_j}{\|\mathbf{r}_j\|}, & U^{(1)}(\mathbf{r}) &= -\mathcal{G} \left(\frac{m_1 m_2}{\|\mathbf{r}_1 - \mathbf{r}_2\|} + \frac{m_1 m_3}{\|\mathbf{r}_1 - \mathbf{r}_3\|} + \frac{m_2 m_3}{\|\mathbf{r}_2 - \mathbf{r}_3\|} \right). \end{aligned}$$

The plane set of Poincaré's canonical variables is introduced as

$$\begin{aligned} \Lambda_j &= \frac{m_0 m_j}{m_0 + m_j} \sqrt{\mathcal{G}(m_0 + m_j) a_j}, & \lambda_j &= M_j + \omega_j, \\ \xi_j &= \sqrt{2\Lambda_j} \sqrt{1 - \sqrt{1 - e_j^2}} \cos \omega_j, & \eta_j &= -\sqrt{2\Lambda_j} \sqrt{1 - \sqrt{1 - e_j^2}} \sin \omega_j, \end{aligned} \quad (2)$$

for $j = 1, 2, 3$, where a_j, e_j, M_j and ω_j are the semi-major axis, the eccentricity, the mean anomaly and the perihelion argument, respectively, of the j -th planet. One immediately sees that both ξ_j and η_j are of the same order of magnitude as the eccentricity e_j . Using Poincaré's variables (2), the Hamiltonian F can be rearranged so that one has

$$F(\mathbf{\Lambda}, \mathbf{\lambda}, \mathbf{\xi}, \mathbf{\eta}) = F^{(0)}(\mathbf{\Lambda}) + F^{(1)}(\mathbf{\Lambda}, \mathbf{\lambda}, \mathbf{\xi}, \mathbf{\eta}), \quad (3)$$

where $F^{(0)} = T^{(0)} + U^{(0)}$, $F^{(1)} = T^{(1)} + U^{(1)}$. Let us emphasize that $F^{(0)} = \mathcal{O}(1)$ and $F^{(1)} = \mathcal{O}(\mu)$, where the small dimensionless parameter $\mu = \max\{m_1/m_0, m_2/m_0, m_3/m_0\}$ highlights the different size of the terms appearing in the Hamiltonian. Therefore, let us remark that the time derivative of each coordinate is $\mathcal{O}(\mu)$ but in the case of the angles

¹Let us stress that the four bodies have the same masses as Sun, Jupiter, Saturn and Uranus, but the orbits studied here are significantly different with respect to the real ones.

$\boldsymbol{\lambda}$. Thus, according to the common language in Celestial Mechanics, in the following we will refer to $\boldsymbol{\lambda}$ and to their conjugate actions $\boldsymbol{\Lambda}$ as the *fast variables*, while $(\boldsymbol{\xi}, \boldsymbol{\eta})$ will be called *secular variables*.

We proceed now by expanding the Hamiltonian (3) in order to construct the first basic approximation of the normal form for elliptic tori. After having chosen a center value $\boldsymbol{\Lambda}^*$ for the Taylor expansions with respect to the fast actions (in a way we will explain later), we perform a translation $\mathcal{T}_{\boldsymbol{\Lambda}^*}$ defined as

$$L_j = \Lambda_j - \Lambda_j^*, \quad \forall j = 1, 2, 3. \quad (4)$$

This is a canonical transformation that leaves the coordinates $\boldsymbol{\lambda}$, $\boldsymbol{\xi}$ and $\boldsymbol{\eta}$ unchanged. The transformed Hamiltonian $\mathcal{H}^{(\mathcal{T})} = F \circ \mathcal{T}_{\boldsymbol{\Lambda}^*}$ can be expanded in power series of \boldsymbol{L} , $\boldsymbol{\xi}$, $\boldsymbol{\eta}$ around the origin. Thus, forgetting an unessential constant we rearrange the Hamiltonian of the system as

$$\mathcal{H}^{(\mathcal{T})}(\boldsymbol{L}, \boldsymbol{\lambda}, \boldsymbol{\xi}, \boldsymbol{\eta}) = \boldsymbol{n}^* \cdot \boldsymbol{L} + \sum_{j_1=2}^{\infty} h_{j_1,0}^{(\text{Kep})}(\boldsymbol{L}) + \sum_{j_1=0}^{\infty} \sum_{j_2=0}^{\infty} h_{j_1,j_2}^{(\mathcal{T})}(\boldsymbol{L}, \boldsymbol{\lambda}, \boldsymbol{\xi}, \boldsymbol{\eta}), \quad (5)$$

where the functions $h_{j_1,j_2}^{(\mathcal{T})}$ are homogeneous polynomials of degree j_1 in the actions \boldsymbol{L} and of degree j_2 in the secular variables $(\boldsymbol{\xi}, \boldsymbol{\eta})$. The coefficients of such homogeneous polynomials do depend analytically and periodically on the angles $\boldsymbol{\lambda}$. The terms $h_{j_1,0}^{(\text{Kep})}$ of the Keplerian part are homogeneous polynomials of degree j_1 in the actions \boldsymbol{L} , the explicit expression of which can be determined in a straightforward manner. In the latter equation the term which is both linear in the actions and independent of all the other canonical variables (i.e., $\boldsymbol{n}^* \cdot \boldsymbol{L}$) has been separated in view of its relevance in perturbation theory, as it will be discussed in the next section. We also expand the coefficients of the power series $h_{j_1,j_2}^{(\mathcal{T})}$ in Fourier series of the angles $\boldsymbol{\lambda}$. The expansion of the Hamiltonian is a traditional procedure in Celestial Mechanics. We work out these expansions for the case of the planar SJSU system using a specially devised algebraic manipulator. The calculation is based on the approach described in sect. 2.1 of [35], which in turn uses the scheme sketched in sect. 3.3 of [45].

The reduction to the planar case is performed as follows. We pick from table IV of [47] the initial conditions of the planets in terms of heliocentric positions and velocities at the Julian Date 2440400.5. Next, we calculate the corresponding orbital elements with respect to the invariant plane (that is perpendicular to the total angular momentum). Finally we include the longitudes of the nodes Ω_j (which are meaningless in the planar case) in the corresponding perihelion longitude ω_j and we eliminate the inclinations by setting them equal to zero. The remaining initial values of the orbital elements are reported in table 1.

Having fixed the initial conditions we come to determining the *average* values (a_1^*, a_2^*, a_3^*) of the semi-major axes during the evolution. To this end we perform a long-term numerical integration of Newton's equations starting from the initial conditions related to the data reported in table 1. After having computed (a_1^*, a_2^*, a_3^*) , we determine the values $\boldsymbol{\Lambda}^*$ via the first equation in (2). This allows us to perform the expansion (5) of the Hamiltonian as a function of the canonical coordinates $(\boldsymbol{L}, \boldsymbol{\lambda}, \boldsymbol{\xi}, \boldsymbol{\eta})$. In our calculations

Table 1: Masses m_j and initial conditions for Jupiter, Saturn and Uranus in our planar model. We adopt the AU as unit of length, the year as time unit and set the gravitational constant $\mathcal{G} = 1$. With these units, the solar mass is equal to $(2\pi)^2$. The initial conditions are expressed by the usual heliocentric planar orbital elements: the semi-major axis a_j , the mean anomaly M_j , the eccentricity e_j and the perihelion longitude ω_j . The data are taken by JPL at the Julian Date 2440400.5.

	Jupiter ($j = 1$)	Saturn ($j = 2$)	Uranus ($j = 3$)
m_j	$(2\pi)^2/1047.355$	$(2\pi)^2/3498.5$	$(2\pi)^2/22902.98$
a_j	5.20463727204700266	9.54108529142232165	19.2231635458410572
M_j	3.04525729444853654	5.32199311882584869	0.19431922829271914
e_j	0.04785365972484999	0.05460848595674678	0.04858667407651962
ω_j	0.24927354029554571	1.61225062288036902	2.99374344439246487

we truncate this initial expansion as follows. (a) The Keplerian part is expanded up to the quartic terms. The series where the general summand $h_{j_1, j_2}^{(\mathcal{T})}$ appears are truncated so to include: (b1) all terms having degree j_1 in the actions \mathbf{L} with $j_1 \leq 3$, (b2) all terms having degree j_2 in the secular variables $(\boldsymbol{\xi}, \boldsymbol{\eta})$, with j_2 such that $2j_1 + j_2 \leq 8$, (b3) all terms up to the trigonometric degree 18 with respect to the angles $\boldsymbol{\lambda}$. This choice is motivated by the remark that the orbits on elliptic tori reach values of the eccentricities smaller than those attained by the real motions (let us recall that both $\xi_j = \mathcal{O}(e_j)$ and $\eta_j = \mathcal{O}(e_j) \forall j = 1, 2, 3$); moreover, larger limits on the fast angles are needed, in order to give a sharp enough numerical evidence of the convergence of the algorithm described in the next section.

Let us now focus on the average with respect to the fast angles of the Hamiltonian written in (5), i.e., $\langle \mathcal{H}^{(\mathcal{T})} \rangle_{\boldsymbol{\lambda}}$. The fast actions \mathbf{L} are obviously invariant with respect to the flow of $\langle \mathcal{H}^{(\mathcal{T})} \rangle_{\boldsymbol{\lambda}}$, thus, they can be neglected inasmuch as the secular motions are considered. The remaining most significant term is given by the lowest order approximation of the secular Hamiltonian, namely its quadratic part $\langle h_{0,2}^{(\mathcal{T})} \rangle_{\boldsymbol{\lambda}}$ which is essentially the one considered in the theory first developed by Lagrange (see [23]) and further improved by Laplace (see [26], [27] and [28]) and by Lagrange himself (see [24], [25]). In modern language, we can say that the origin $(\boldsymbol{\xi}, \boldsymbol{\eta}) = (\mathbf{0}, \mathbf{0})$ of the secular coordinates is an elliptic equilibrium point for the secular Hamiltonian. It is well known that under mild assumptions on the quadratic part of the Hamiltonian which are satisfied in our case (see sect. 3 of [5] where such hypotheses are shown to be generically fulfilled for a planar model of our Solar System) one can find a canonical transformation $(\mathbf{L}, \boldsymbol{\lambda}, \boldsymbol{\xi}, \boldsymbol{\eta}) = \mathcal{D}(\mathbf{p}, \mathbf{q}, \mathbf{x}, \mathbf{y})$ with the following properties: (i) $\mathbf{L} = \mathbf{p}$ and $\boldsymbol{\lambda} = \mathbf{q}$, (ii) the map $(\boldsymbol{\xi}, \boldsymbol{\eta}) = (\boldsymbol{\xi}(\mathbf{x}), \boldsymbol{\eta}(\mathbf{y}))$ is linear, (iii) \mathcal{D} diagonalizes the quadratic part of the Hamiltonian, so that we can write $\langle h_{0,2}^{(\mathcal{T})} \rangle_{\boldsymbol{\lambda}}$ in the new coordinates as $\sum_{j=1}^3 \nu_j^{(0)} (x_j^2 + y_j^2)/2$, where all the entries of the vector $\boldsymbol{\nu}^{(0)}$ have the same sign. Our algorithm constructing a suitable normal form for elliptic

tori starts from the Hamiltonian $H^{(0)} = \mathcal{H}^{(\mathcal{T})} \circ \mathcal{D}$, i.e.,

$$H^{(0)}(\mathbf{p}, \mathbf{q}, \mathbf{x}, \mathbf{y}) = \mathcal{H}^{(\mathcal{T})}(\mathcal{D}(\mathbf{p}, \mathbf{q}, \mathbf{x}, \mathbf{y})). \quad (6)$$

3 Formal Algorithm

We present the formal algorithm making reference to a generic Hamiltonian with $n_1 + n_2$ degrees of freedom, where the canonical coordinates $(\mathbf{p}, \mathbf{q}, \mathbf{x}, \mathbf{y})$ can naturally be split in two parts, that are $(\mathbf{p}, \mathbf{q}) \in \mathbb{R}^{n_1} \times \mathbb{T}^{n_1}$ and $(\mathbf{x}, \mathbf{y}) \in \mathbb{R}^{n_2} \times \mathbb{R}^{n_2}$.

Our aim is to determine a canonical transformation $(\mathbf{p}, \mathbf{q}, \mathbf{x}, \mathbf{y}) = \mathcal{K}^{(\infty)}(\mathbf{P}, \mathbf{Q}, \mathbf{X}, \mathbf{Y})$ which gives the Hamiltonian $H^{(\infty)} = H^{(0)} \circ \mathcal{K}^{(\infty)}$ the normal form²

$$H^{(\infty)}(\mathbf{P}, \mathbf{Q}, \mathbf{X}, \mathbf{Y}) = \boldsymbol{\omega}^{(\infty)} \cdot \mathbf{P} + \sum_{j=1}^{n_2} \frac{\Omega_j^{(\infty)} (X_j^2 + Y_j^2)}{2} + \mathcal{O}(\|\mathbf{P}\|^2) + \mathcal{O}(\|\mathbf{P}\| \|\mathbf{X}, \mathbf{Y}\|) + \mathcal{O}(\|\mathbf{X}, \mathbf{Y}\|^3). \quad (7)$$

Here the notation means that we want to remove all terms which are linear in \mathbf{P} and independent of (\mathbf{X}, \mathbf{Y}) , or at most quadratic in (\mathbf{X}, \mathbf{Y}) and independent of \mathbf{P} . A solution of the Hamilton's equations is

$$(\mathbf{P}(t), \mathbf{Q}(t), \mathbf{X}(t), \mathbf{Y}(t)) = (\mathbf{0}, \mathbf{Q}_0 + \boldsymbol{\omega}^{(\infty)} t, \mathbf{0}, \mathbf{0}). \quad (8)$$

Choosing the initial conditions $(\mathbf{P}, \mathbf{Q}, \mathbf{X}, \mathbf{Y}) = (\mathbf{0}, \mathbf{Q}_0, \mathbf{0}, \mathbf{0})$ (with $\mathbf{Q}_0 \in \mathbb{T}^{n_1}$), one immediately sees that the corresponding orbit lies on the invariant n_1 -dimensional torus $\mathbf{P} = \mathbf{0}$ and $\mathbf{X} = \mathbf{Y} = \mathbf{0}$ and that the orbits are quasi-periodic on it with frequencies $\boldsymbol{\omega}^{(\infty)}$.

The generic r -th step of our normalization algorithm is performed as follows. We reorder the Hamiltonian as

$$H^{(r-1)}(\mathbf{p}, \mathbf{q}, \mathbf{x}, \mathbf{y}) = \boldsymbol{\omega}^{(r-1)} \cdot \mathbf{p} + \boldsymbol{\Omega}^{(r-1)} \cdot \mathbf{J} + \sum_{s=0}^{\infty} \sum_{l=0}^{\infty} \sum_{\substack{2j_1+j_2=l \\ j_1 \geq 0, j_2 \geq 0}} f_{j_1, j_2}^{(r-1, s)}(\mathbf{p}, \mathbf{q}, \mathbf{x}, \mathbf{y}), \quad (9)$$

where $J_j = (x_j^2 + y_j^2)/2$ is the action which is usually related to the j -th pair of secular canonical coordinates (x_j, y_j) , $\forall j = 1, \dots, n_2$. Moreover we pick a suitable integer $K > 0$ and determine the functions $f_{j_1, j_2}^{(r-1, s)}$ so that they satisfy the following rules:

- (A) $f_{j_1, j_2}^{(r-1, s)} \in \mathcal{P}_{j_1, j_2}^{(sK)}$, where $\mathcal{P}_{j_1, j_2}^{(sK)}$ is the class of functions which are homogeneous polynomials of degree j_1 in the actions \mathbf{p} , homogeneous polynomials of degree j_2 in the secular variables (\mathbf{x}, \mathbf{y}) , and trigonometric polynomials of degree sK in the angles \mathbf{q} ;

²We introduce a minor change of notations, using the symbol $\boldsymbol{\omega}$ for the frequency vector related to the motion on a torus and $\boldsymbol{\Omega}$ for the frequencies of the oscillations transverse to the elliptic torus. The reader should avoid confusion with the previous use, when $\boldsymbol{\omega}$ and $\boldsymbol{\Omega}$ denoted the longitudes of the perihelia and of the nodes, respectively, which is the classical notation in Celestial Mechanics.

- (B) the terms $f_{j_1, j_2}^{(r-1, s)}$ are “well Fourier-ordered”; this nonstandard definition means that $\forall j_1 \geq 0, j_2 \geq 0, s \geq 1$ every Fourier harmonic \mathbf{k} appearing in the expansion of $f_{j_1, j_2}^{(r-1, s)}$ is such that its corresponding trigonometric degree $|\mathbf{k}| = |k_1| + \dots + |k_{n_1}|$ satisfies $(s-1)K < |\mathbf{k}| \leq sK$.

By using formula (5) and the properties (i)–(iii) of the canonical transformation \mathcal{D} , one easily sees that the Hamiltonian $H^{(0)}$ defined in (6) can be expanded in the form written in (9), after having suitably reordered its Fourier expansion so to satisfy the above requirements (A) and (B). Therefore, our constructive algorithm can be applied to the Hamiltonian $H^{(0)}$ by starting with $r = 1$.

The comparison of the expansion in (9) with the normal form in (7) clearly shows that we should remove all terms $f_{j_1, j_2}^{(0, s)}$ where the index $l = 2j_1 + j_2$ is such that $0 \leq l \leq 2$. Thus, the r -th step of our algorithm can be naturally divided in three stages, each one aiming to reduce the perturbation terms with $l = 0, 1, 2$, respectively.

3.1 First Stage of the Normalization Step

The aim of the first stage in the r -th normalization step is to remove the terms depending only on \mathbf{q} .

We use the Lie series algorithm to calculate the canonical transformations (see, e.g., [12] for an introduction). The generating function $\chi_0^{(r)}(\mathbf{q}) \in \mathcal{P}_{0,0}^{(rK)}$ is determined by solving the equation

$$\left\{ \chi_0^{(r)}, \boldsymbol{\omega}^{(r-1)} \cdot \mathbf{p} \right\} + \sum_{s=1}^r f_{0,0}^{(r-1, s)}(\mathbf{q}) = 0, \quad (10)$$

and the new Hamiltonian is determined as $H^{(1;r)} = \exp \mathcal{L}_{\chi_0^{(r)}} H^{(r-1)}$, the symbol $\{\cdot, \cdot\}$ denoting the Poisson bracket. The equation for the generating function admits a solution provided the frequency vector $\boldsymbol{\omega}^{(r-1)}$ is non-resonant up to order rK . More precisely, we assume that

$$\min_{0 < |\mathbf{k}| \leq rK} |\mathbf{k} \cdot \boldsymbol{\omega}^{(r-1)}| \geq \alpha_r \quad \text{with } \alpha_r > 0, \quad (11)$$

where $\{\alpha_r\}_{r>0}$ is a sequence of real positive numbers and $|\mathbf{k}| = |k_1| + \dots + |k_{n_1}|$. The solution of the homological equation (10) can be easily recovered by looking at the little more complicate case of $X_2^{(r)}$, which is discussed in the third stage of the r -th normalization step (see formulas (21)–(22)).

The canonical transformation writes $(\mathbf{p}, \mathbf{q}, \mathbf{x}, \mathbf{y}) = \exp \mathcal{L}_{\chi_0^{(r)}}(\mathbf{p}', \mathbf{q}', \mathbf{x}', \mathbf{y}')$. Omitting primes in order to simplify the notations the transformed Hamiltonian can be written as

$$H^{(1;r)}(\mathbf{p}, \mathbf{q}, \mathbf{x}, \mathbf{y}) = \boldsymbol{\omega}^{(r-1)} \cdot \mathbf{p} + \boldsymbol{\Omega}^{(r-1)} \cdot \mathbf{J} + \sum_{s=0}^{\infty} \sum_{l=0}^{\infty} \sum_{\substack{2j_1+j_2=l \\ j_1 \geq 0, j_2 \geq 0}} f_{j_1, j_2}^{(1;r, s)}(\mathbf{p}, \mathbf{q}, \mathbf{x}, \mathbf{y}). \quad (12)$$

The functions $f_{j_1, j_2}^{(1;r, s)}$ are recursively defined, we omit this lengthy calculation since it is straightforward. The main remark is concerned with the classes of functions. It is easy

to check that

$$\frac{1}{i!} \mathcal{L}_{\chi_0}^i f_{j_1, j_2}^{(r-1, s)} \in \mathcal{P}_{j_1-i, j_2}^{((s+ir)K)} \quad \forall 0 \leq i \leq j_1, j_2 \geq 0, s \geq 0, \quad (13)$$

but it does not satisfy condition (B) at the beginning of the present section. Therefore, after having constructed $\sum_{j=0}^{s+ir} f_{j_1-i, j_2}^{(1; r, j)}$ by calculating all Poisson brackets in $\frac{1}{i!} \mathcal{L}_{\chi_0}^i f_{j_1, j_2}^{(r-1, s)}$, we perform a suitable reordering of the Taylor-Fourier series, so that the expansion (12) satisfies both conditions (A) and (B).

3.2 Second Stage of the Normalization Step

The aim of the second stage of the r -th normalization step is to remove the terms which are linear in (\mathbf{x}, \mathbf{y}) and independent of \mathbf{p} .

We construct a second generating function $\chi_1^{(r)}(\mathbf{q}, \mathbf{x}, \mathbf{y}) \in \mathcal{P}_{0,1}^{(rK)}$ by solving the equation

$$\left\{ \chi_1^{(r)}, \boldsymbol{\omega}^{(r-1)} \cdot \mathbf{p} + \sum_{j=1}^{n_2} \frac{\Omega_j^{(r-1)}}{2} (x_j^2 + y_j^2) \right\} + \sum_{s=0}^r f_{0,1}^{(1; r, s)}(\mathbf{q}, \mathbf{x}, \mathbf{y}) = 0. \quad (14)$$

With this generating function we construct the new Hamiltonian $H^{(II; r)} = \exp \mathcal{L}_{\chi_1^{(r)}} H^{(I; r)}$.

Let us show how equation (14) is solved. It is convenient to temporarily introduce action-angle coordinates in place of the secular pairs (\mathbf{x}, \mathbf{y}) by putting $x_j = \sqrt{2J_j} \cos \varphi_j$ and $y_j = \sqrt{2J_j} \sin \varphi_j \forall j = 1, \dots, n_2$, so that the expansion of the known terms appearing in equation (14) has the form:

$$\sum_{s=0}^r f_{0,1}^{(1; r, s)}(\mathbf{q}, \mathbf{J}, \boldsymbol{\varphi}) = \sum_{0 \leq |\mathbf{k}| \leq rK} \sum_{j=1}^{n_2} \sqrt{2J_j} \left[c_{\mathbf{k}, j}^{(\pm)} \cos(\mathbf{k} \cdot \mathbf{q} \pm \varphi_j) + d_{\mathbf{k}, j}^{(\pm)} \sin(\mathbf{k} \cdot \mathbf{q} \pm \varphi_j) \right], \quad (15)$$

with known real coefficients $c_{\mathbf{k}, j}^{(\pm)}$ and $d_{\mathbf{k}, j}^{(\pm)}$. Thus, one can easily check that

$$\chi_1^{(r)}(\mathbf{q}, \mathbf{J}, \boldsymbol{\varphi}) = \sum_{0 \leq |\mathbf{k}| \leq rK} \sum_{j=1}^{n_2} \sqrt{2J_j} \left[-\frac{c_{\mathbf{k}, j}^{(\pm)} \sin(\mathbf{k} \cdot \mathbf{q} \pm \varphi_j)}{\mathbf{k} \cdot \boldsymbol{\omega}^{(r-1)} \pm \Omega_j^{(r-1)}} + \frac{d_{\mathbf{k}, j}^{(\pm)} \cos(\mathbf{k} \cdot \mathbf{q} \pm \varphi_j)}{\mathbf{k} \cdot \boldsymbol{\omega}^{(r-1)} \pm \Omega_j^{(r-1)}} \right] \quad (16)$$

is a solution of the homological equation (14), and it is consistently constructed provided the frequency vector $\boldsymbol{\omega}^{(r-1)}$ satisfies the so-called *first Melnikov non-resonance condition* up to order rK , i.e.,

$$\min_{\substack{0 \leq |\mathbf{k}| \leq rK \\ j=1, \dots, n_2}} |\mathbf{k} \cdot \boldsymbol{\omega}^{(r-1)} \pm \Omega_j^{(r-1)}| \geq \alpha_r \quad \text{with } \alpha_r > 0, \quad (17)$$

and all the entries of the frequency vector $\boldsymbol{\Omega}^{(r-1)}$ are far enough from the origin, i.e.,

$$\min_{j=1, \dots, n_2} |\Omega_j^{(r-1)}| \geq \beta \quad \text{with } \beta > 0. \quad (18)$$

We remark that the latter condition (18) is needed in general, but it is not necessary in the case of a planetary Hamiltonian. For, d'Alembert rules hold true, and so all coefficients $c_{\mathbf{k},j}^{(\pm)}$ and $d_{\mathbf{k},j}^{(\pm)}$ appearing in (15) and having even values of $|\mathbf{k}|$ are equal to zero. However, such condition is substantially included in a further one (i.e., (31)) that we will need to introduce later.

Starting from the expansion (16) of $\chi_1^{(r)}(\mathbf{q}, \mathbf{J}, \boldsymbol{\varphi})$, one can immediately recover the expression of $\chi_1^{(r)}(\mathbf{q}, \mathbf{x}, \mathbf{y})$ as a function of the original polynomial variables. We can then explicitly calculate the expansion of the new Hamiltonian, which is written as

$$H^{(\text{II};r)}(\mathbf{p}, \mathbf{q}, \mathbf{x}, \mathbf{y}) = \boldsymbol{\omega}^{(r-1)} \cdot \mathbf{p} + \boldsymbol{\Omega}^{(r-1)} \cdot \mathbf{J} + \sum_{s=0}^{\infty} \sum_{l=0}^{\infty} \sum_{\substack{2j_1+j_2=l \\ j_1 \geq 0, j_2 \geq 0}} f_{j_1, j_2}^{(\text{II};r,s)}(\mathbf{p}, \mathbf{q}, \mathbf{x}, \mathbf{y}). \quad (19)$$

Here too we omit the explicit recursive expressions of the terms $f_{j_1, j_2}^{(\text{II};r,s)}$, which can be obtained by a quite annoying calculation. We just add a remark on the implementation via computer algebra. Let us remark that

$$\frac{1}{i!} \mathcal{L}_{\chi_1^{(r)}}^i \sum_{2j_1+j_2=l} f_{j_1, j_2}^{(\text{I};r,s)} \in \bigcup_{2j_1+j_2=l-i} \mathcal{P}_{j_1, j_2}^{(s+ir)K} \quad \forall 0 \leq i \leq l, \quad s \geq 0. \quad (20)$$

Therefore we construct the sum $\sum_{j=0}^{s+ir} \sum_{2j_1+j_2=l-i} f_{j_1, j_2}^{(\text{II};r,j)}$ by calculating all the Poisson brackets appearing in the expression of $\frac{1}{i!} \mathcal{L}_{\chi_1^{(r)}}^i \sum_{2j_1+j_2=l} f_{j_1, j_2}^{(\text{I};r,s)}$ and then we proceed again with a reordering of the Taylor-Fourier series so that also the expansion (19) satisfies the conditions (A) and (B), which have been stated at the beginning of the present section.

3.3 Third Stage of the Normalization Step

The third and last stage of the r -th normalization step is more elaborated. The aim is to remove two classes of terms, namely terms which are linear in \mathbf{p} and independent of (\mathbf{x}, \mathbf{y}) , and terms which are quadratic in (\mathbf{x}, \mathbf{y}) and independent of \mathbf{p} .

The Hamiltonian produced at the end of the r -th normalization step is provided by the composition of three canonical transformations³ which can be given in terms of Lie series, thus constructing the final Hamiltonian $H^{(r)} = \exp \mathcal{L}_{\mathcal{D}_2^{(r)}} \circ \exp \mathcal{L}_{Y_2^{(r)}} \circ \exp \mathcal{L}_{X_2^{(r)}} H^{(\text{II};r)}$. The generating functions belong to three different classes: $X_2^{(r)}(\mathbf{p}, \mathbf{q}) \in \mathcal{P}_{1,0}^{(rK)}$, $Y_2^{(r)}(\mathbf{q}, \mathbf{x}, \mathbf{y}) \in \mathcal{P}_{0,2}^{(rK)}$ and $\mathcal{D}_2^{(r)}(\mathbf{x}, \mathbf{y}) \in \mathcal{P}_{0,2}^{(0)}$. The explicit expressions of these generating functions are given below, in formulas (23), (26) and (30), respectively.

³When one focuses on the estimates needed to prove the convergence of the algorithm, it is certainly simpler to introduce a single generating function $\chi_2^{(r)}(\mathbf{p}, \mathbf{q}, \mathbf{x}, \mathbf{y}) = X_2^{(r)}(\mathbf{p}, \mathbf{q}) + Y_2^{(r)}(\mathbf{q}, \mathbf{x}, \mathbf{y})$ and to consider the new Hamiltonian $\exp \mathcal{L}_{\mathcal{D}_2^{(r)}} \circ \exp \mathcal{L}_{\chi_2^{(r)}} H^{(\text{II};r)}$ which slightly differs from $H^{(r)}$, because $X_2^{(r)}$, and $Y_2^{(r)}$ do not commute with respect to the Poisson brackets. However, in the present work we prefer to split the present third stage of the r -th normalization step in three parts, so to highlight their different roles. Moreover, this choice looks more natural when one implements the constructive algorithm by algebraic manipulations on a computer.

We start with $X_2^{(r)}(\mathbf{p}, \mathbf{q}) \in \mathcal{P}_{1,0}^{(rK)}$, which is determined as the solution of the equation

$$\left\{ X_2^{(r)}, \boldsymbol{\omega}^{(r-1)} \cdot \mathbf{p} \right\} + \sum_{s=1}^r f_{1,0}^{(\text{II};r,s)}(\mathbf{p}, \mathbf{q}) = 0. \quad (21)$$

Writing the expansion of the known terms appearing in equation (21) in the form

$$\sum_{s=1}^r f_{1,0}^{(\text{II};r,s)}(\mathbf{p}, \mathbf{q}) = \sum_{0 < |\mathbf{k}| \leq rK} \sum_{j=1}^{n_1} p_j [c_{\mathbf{k},j} \cos(\mathbf{k} \cdot \mathbf{q}) + d_{\mathbf{k},j} \sin(\mathbf{k} \cdot \mathbf{q})], \quad (22)$$

with known real coefficients $c_{\mathbf{k},j}$ and $d_{\mathbf{k},j}$ the generating function is given by

$$X_2^{(r)}(\mathbf{p}, \mathbf{q}) = \sum_{0 < |\mathbf{k}| \leq rK} \sum_{j=1}^{n_1} p_j \left[-\frac{c_{\mathbf{k},j} \sin(\mathbf{k} \cdot \mathbf{q})}{\mathbf{k} \cdot \boldsymbol{\omega}^{(r-1)}} + \frac{d_{\mathbf{k},j} \cos(\mathbf{k} \cdot \mathbf{q})}{\mathbf{k} \cdot \boldsymbol{\omega}^{(r-1)}} \right], \quad (23)$$

The latter expression is consistent if the frequency vector $\boldsymbol{\omega}^{(r-1)}$ satisfies the non-resonance condition (11).

The generating function $Y_2^{(r)}(\mathbf{q}, \mathbf{x}, \mathbf{y}) \in \mathcal{P}_{0,2}^{(rK)}$ is determined by solving the equation

$$\left\{ Y_2^{(r)}, \boldsymbol{\omega}^{(r-1)} \cdot \mathbf{p} + \sum_{j=1}^{n_2} \frac{\Omega_j^{(r-1)}}{2} (x_j^2 + y_j^2) \right\} + \sum_{s=1}^r f_{0,2}^{(\text{II};r,s)}(\mathbf{q}, \mathbf{x}, \mathbf{y}) = 0. \quad (24)$$

Proceeding as in the second stage we use action-angle variables $(\mathbf{J}, \boldsymbol{\varphi})$ in place of the secular pairs (\mathbf{x}, \mathbf{y}) , so that the expansion of the known terms appearing in equation (24) takes the form

$$\sum_{s=1}^r f_{0,2}^{(\text{II};r,s)}(\mathbf{q}, \mathbf{J}, \boldsymbol{\varphi}) = \sum_{0 < |\mathbf{k}| \leq rK} \sum_{i,j=1}^{n_2} 2\sqrt{J_i J_j} \left[c_{\mathbf{k},i,j}^{(\pm,\pm)} \cos(\mathbf{k} \cdot \mathbf{q} \pm \varphi_i \pm \varphi_j) + d_{\mathbf{k},i,j}^{(\pm,\pm)} \sin(\mathbf{k} \cdot \mathbf{q} \pm \varphi_i \pm \varphi_j) \right], \quad (25)$$

with known real coefficients $c_{\mathbf{k},i,j}^{(\pm,\pm)}$ and $d_{\mathbf{k},i,j}^{(\pm,\pm)}$. Hence the generating function is determined as

$$Y_2^{(r)}(\mathbf{q}, \mathbf{J}, \boldsymbol{\varphi}) = \sum_{0 < |\mathbf{k}| \leq rK} \sum_{i,j=1}^{n_2} 2\sqrt{J_i J_j} \left[-\frac{c_{\mathbf{k},i,j}^{(\pm,\pm)} \sin(\mathbf{k} \cdot \mathbf{q} \pm \varphi_i \pm \varphi_j)}{\mathbf{k} \cdot \boldsymbol{\omega}^{(r-1)} \pm \Omega_i^{(r-1)} \pm \Omega_j^{(r-1)}} + \frac{d_{\mathbf{k},i,j}^{(\pm,\pm)} \cos(\mathbf{k} \cdot \mathbf{q} \pm \varphi_i \pm \varphi_j)}{\mathbf{k} \cdot \boldsymbol{\omega}^{(r-1)} \pm \Omega_i^{(r-1)} \pm \Omega_j^{(r-1)}} \right]. \quad (26)$$

In order to make this expression consistent we must assume that the frequency vector $\boldsymbol{\omega}^{(r-1)}$ satisfies the so-called *second Melnikov non-resonance condition* up to order rK , i.e.,

$$\min_{\substack{0 < |\mathbf{k}| \leq rK \\ i,j=1,\dots,n_2}} |\mathbf{k} \cdot \boldsymbol{\omega}^{(r-1)} \pm \Omega_i^{(r-1)} \pm \Omega_j^{(r-1)}| \geq \alpha_r \quad \text{with } \alpha_r > 0. \quad (27)$$

Let us here remark that the latter condition includes also the non-resonance condition (11) as a special case, i.e., when $i = j$ and the signs appearing in the expression $\pm\Omega_i^{(r-1)} \pm\Omega_j^{(r-1)}$ are opposite.

Concerning the the generating function $\mathcal{D}_2^{(r)}$, once again it is convenient to replace the secular pairs (\mathbf{x}, \mathbf{y}) with the action-angle coordinates $(\mathbf{J}, \boldsymbol{\varphi})$. Remark that $\boldsymbol{\Omega}^{(r-1)} \cdot \mathbf{J}$ and $f_{0,2}^{(\text{II};r,0)}(\mathbf{x}, \mathbf{y})$ are the only terms appearing in expansion (19) which are quadratic in (\mathbf{x}, \mathbf{y}) (so they also are $\mathcal{O}(\mathbf{J})$) and do not depend on \mathbf{p} and \mathbf{q} . The canonical transformation induced by the Lie series $\exp \mathcal{L}_{\mathcal{D}_2^{(r)}}$ aims to eliminate the part of $f_{0,2}^{(\text{II};r,0)}$ depending on the secular angles $\boldsymbol{\varphi}$. Therefore, the generating function $\mathcal{D}_2^{(r)}$ is determined as the solution of the equation

$$\left\{ \mathcal{D}_2^{(r)}, \boldsymbol{\Omega}^{(r-1)} \cdot \mathbf{J} \right\} + f_{0,2}^{(\text{II};r,0)}(\mathbf{J}, \boldsymbol{\varphi}) - \langle f_{0,2}^{(\text{II};r,0)} \rangle_{\boldsymbol{\varphi}} = 0, \quad (28)$$

where $\langle \cdot \rangle_{\boldsymbol{\varphi}}$ denotes the average with respect to the angles $\boldsymbol{\varphi}$. Writing the expansion of the known terms as

$$f_{0,2}^{(\text{II};r,0)}(\mathbf{J}, \boldsymbol{\varphi}) = \sum_{i,j=1}^{n_2} \sum_{\substack{s_i=\pm 1 \\ s_j=\pm 1}} 2\sqrt{J_i J_j} \left[c_{i,j,s_i,s_j} \cos(s_i\varphi_i + s_j\varphi_j) + d_{i,j,s_i,s_j} \sin(s_i\varphi_i + s_j\varphi_j) \right], \quad (29)$$

with known real coefficients c_{i,j,s_i,s_j} and d_{i,j,s_i,s_j} the generating function is given by

$$\mathcal{D}_2^{(r)}(\mathbf{J}, \boldsymbol{\varphi}) = \sum_{i,j=1}^{n_2} \sum_{\substack{s_i,s_j=\pm 1 \\ i \cdot s_i + j \cdot s_j \neq 0}} 2\sqrt{J_i J_j} \left[-\frac{c_{i,j,s_i,s_j} \sin(s_i\varphi_i + s_j\varphi_j)}{s_i\Omega_i^{(r-1)} + s_j\Omega_j^{(r-1)}} + \frac{d_{i,j,s_i,s_j} \cos(s_i\varphi_i + s_j\varphi_j)}{s_i\Omega_i^{(r-1)} + s_j\Omega_j^{(r-1)}} \right]. \quad (30)$$

The solution is consistent provided the frequency vector $\boldsymbol{\Omega}^{(r-1)}$ satisfies the finite non-resonance condition

$$\min_{|l|=2} |l \cdot \boldsymbol{\Omega}^{(r-1)}| \geq \beta \quad \text{with } \beta > 0. \quad (31)$$

Having determined the generating functions $Y_2^{(r)}$ and $\mathcal{D}_2^{(r)}$ it is a standard matter to replace the action-angle variables $\mathbf{J}, \boldsymbol{\varphi}$ with the secular variables \mathbf{x}, \mathbf{y} .

At this point of the algorithm, it is convenient to slightly modify the frequencies $\boldsymbol{\omega}^{(r-1)}$ and $\boldsymbol{\Omega}^{(r-1)}$, so to include the terms which are linear with respect to the actions and do not depend on the angles. Such terms can not be eliminated by our normalization procedure. More precisely, we define $\boldsymbol{\omega}^{(r)}$ and $\boldsymbol{\Omega}^{(r)}$, so that

$$\boldsymbol{\omega}^{(r)} \cdot \mathbf{p} = \boldsymbol{\omega}^{(r-1)} \cdot \mathbf{p} + f_{1,0}^{(\text{II};r,0)}(\mathbf{p}), \quad \boldsymbol{\Omega}^{(r)} \cdot \mathbf{J} = \boldsymbol{\Omega}^{(r-1)} \cdot \mathbf{J} + \langle f_{0,2}^{(\text{II};r,0)} \rangle_{\boldsymbol{\varphi}}. \quad (32)$$

We are now able to explicitly produce the expansion of the new Hamiltonian, which can be written as

$$H^{(r)}(\mathbf{p}, \mathbf{q}, \mathbf{x}, \mathbf{y}) = \boldsymbol{\omega}^{(r)} \cdot \mathbf{p} + \boldsymbol{\Omega}^{(r)} \cdot \mathbf{J} + \sum_{s=0}^{\infty} \sum_{l=0}^{\infty} \sum_{\substack{2j_1+j_2=l \\ j_1 \geq 0, j_2 \geq 0}} f_{j_1, j_2}^{(r,s)}(\mathbf{p}, \mathbf{q}, \mathbf{x}, \mathbf{y}). \quad (33)$$

Let us remark that this expansion of $H^{(r)}$ has exactly the same form of that written for $H^{(r-1)}$ in (9), but we stress that the algorithm is arranged so to make smaller and smaller the contribution of the terms $f_{j_1, j_2}^{(r,s)}$, when the value of r is increased, $\forall s \geq 0$ and $l = 2j_1 + j_2 = 0, 1, 2$.

Let us add a remark which may be useful in implementing the transformation via computer algebra. For what concerns the generating function $X_2^{(r)}$ we have

$$\frac{1}{i!} \mathcal{L}_{X_2^{(r)}}^i f_{j_1, j_2}^{(\text{II}; r, s)} \in \mathcal{P}_{j_1, j_2}^{((s+ir)K)} \quad \forall i \geq 0, j_1 \geq 0, j_2 \geq 0, s \geq 0. \quad (34)$$

For the generating function $Y_2^{(r)}$ we have the relations

$$\frac{1}{i!} \mathcal{L}_{Y_2^{(r)}}^i \sum_{2j_1+j_2=l} f_{j_1, j_2}^{(\text{II}; r, s)} \in \bigcup_{2j_1+j_2=l} \mathcal{P}_{j_1, j_2}^{((s+ir)K)} \quad \forall i \geq 0, l \geq 0, s \geq 0. \quad (35)$$

Finally, one can easily remark that each class of function is invariant with respect to a Poisson bracket with the generating function $\mathcal{D}_2^{(r)}$. Hence we have

$$\frac{1}{i!} \mathcal{L}_{\mathcal{D}_2^{(r)}}^i f_{j_1, j_2}^{(\text{II}; r, s)} \in \mathcal{P}_{j_1, j_2}^{(sK)} \quad \forall i \geq 0, j_1 \geq 0, j_2 \geq 0, s \geq 0. \quad (36)$$

By taking into account the relations (34)–(36) among the classes of functions, the definition (32) of the new frequencies vectors and by reordering the Taylor-Fourier series, it is possible to ensure that also the expansion (33) satisfies the conditions (A) and (B) which have been stated at the beginning of the present section.

Thus the r -th step of the normalization procedure that we have described here can be iterated.

3.4 Some Remarks about the Convergence of the Normalization Algorithm

We devote this section to an informal discussion of the relations between the normalization procedure for an elliptic torus, which is the subject of the present paper, and the Kolmogorov's algorithm for a torus of maximal dimension. Our aim is to bring into evidence, on the one hand, the differences that make the case of an elliptic lower dimensional torus definitely more difficult and, on the other hand, the impact that these differences have on the explicit calculation.

The main hypotheses of Kolmogorov's theorem are (a) that the perturbation should be small enough and (b) that a strong non-resonance condition must be satisfied by the

frequencies of the unperturbed torus. Both these conditions appear also in the proof of existence of elliptic tori, but the condition of non-resonance presents some critical peculiarities.

A common problem in perturbation theory is concerned with the smallness of the perturbation, because the main analytical estimates are usually extremely restrictive. Nevertheless, we have strong evidence that realistic estimates may be obtained by using algebraic manipulations in order to implement a computer-assisted proof (see, e.g., [35]). In the case of Kolmogorov's theorem a computer-assisted procedure takes advantage of the preliminary application of the algorithm constructing the normal form (which is explicitly performed for a *finite* number of steps R , as large as possible), because a suitable version of the KAM theorem is finally applied to the Hamiltonian $H^{(R)}$ having the perturbing terms strongly reduced with respect to the initial $H^{(0)}$. In the case of elliptic lower dimensional tori a similar procedure applies. The explicit application of the normalization algorithm mainly requires to translate into a programming language the method described in the previous sections. Concerning the actual reduction of the perturbation, by comparing the Hamiltonian normal form (7) with the expansion (33) of $H^{(r)}$, one easily realizes that the initial expression of the perturbation (making part of the Hamiltonian $H^{(0)}$, written in (6)) is given by

$$\sum_{s=0}^{\infty} \sum_{l=0}^2 \sum_{\substack{2j_1+j_2=l \\ j_1 \geq 0, j_2 \geq 0}} f_{j_1, j_2}^{(0,s)}. \quad (37)$$

Looking at all the preliminary expansions, which have been described in sect. 2 and allowed us to introduce the initial Hamiltonian $H^{(0)}$, one immediately sees that all the perturbing terms appearing in (37) are proportional to μ . Let us also recall that the small parameter μ is equal to the mass ratio between the biggest planet and the central star (according to its definition given in the discussion following formula (3)).

The non-resonance conditions on the frequencies represent a definitely more delicate problem. We recall that in order to apply Kolmogorov's theorem for a maximal dimensional torus, one must choose the n frequencies $\omega_1, \dots, \omega_n$ so as to satisfy a strong non-resonance condition. A typical request is that they obey a Diophantine condition, i.e., that the sequence $\{\alpha_r\}_{r \geq 1}$ appearing in the inequality (11) must be such that $\alpha_r \geq \gamma/(rK)^\tau$ with suitable positive values of the constant γ and τ . This choice must be made at the very beginning of the procedure, and the perturbed invariant torus that is found at the end has *the same* frequencies as the unperturbed one. This is assured by introducing, at every step, a small translation of the actions which keeps the frequencies constant.

In the case of the elliptic lower dimensional torus one deals instead with two separate set of frequencies, namely $\boldsymbol{\omega}^{(0)} \in \mathbb{R}^{n_1}$ which characterize the orbits on the torus, and the transverse frequencies $\boldsymbol{\Omega}^{(0)} \in \mathbb{R}^{n_2}$ that are related to the oscillations of orbits close to but not lying on the torus. Now, the frequencies $\boldsymbol{\omega}^{(0)}$ on the torus can be chosen in an arbitrary way, but the transverse frequencies $\boldsymbol{\Omega}^{(0)}$ are functions of $\boldsymbol{\omega}^{(0)}$, being given by the Hamiltonian. This is easily understood by considering the case of a periodic orbit, i.e., $n_1 = 1$, since in that case the transverse frequencies are related to the eigenvalues of the monodromy matrix.

The striking fact is that, due precisely to the dependence of the transverse frequencies

$\Omega^{(0)}$ on $\omega^{(0)}$, the algorithm forces us to change these frequencies at every step. That is, one actually deals with infinite sequences $\omega^{(r)}$ and $\Omega^{(r)}$, all required to satisfy at every order a non-resonance condition of the form (27). Moreover, both sequences should converge to a final set of frequencies $\omega^{(\infty)} = \omega^{(\infty)}(\omega^{(0)})$ and $\Omega^{(\infty)} = \Omega^{(\infty)}(\omega^{(0)})$ which must be non-resonant (e.g., Diophantine). Thus, we are forced to conclude that, depending on the initial choice of $\omega^{(0)}$, it may happen that the algorithm stops at some step because the frequencies fail to satisfy some of the non-resonance conditions (11), (17), (18), (27) and (31). This is indeed one of the main difficulties in working out the proof of existence of an elliptic torus.

Let us first give an informal description of the analytical procedure. We leave the full exposition with the convergence proof to a forthcoming paper. One initially considers an open ball $\mathcal{B} \subset \mathbb{R}^{n_1}$ such that the Diophantine condition *at finite order* required for the first step is satisfied by every $\omega^{(0)} \in \mathcal{B} \subset \mathbb{R}^{n_1}$ and by the corresponding transverse frequencies $\Omega^{(0)}$. This can be done, because only a finite number of non-resonance relations are considered. One must show that at every step there exists a subset of frequencies in \mathcal{B} which satisfies the non-resonance conditions (still at finite but increasing order) required in order to perform the next step, together with the corresponding transverse frequencies. This is obtained by a procedure which is inspired by Arnold's proof scheme of KAM theorem, and is quite different from Kolmogorov's one (compare [22] with [1]). At every step one removes from \mathcal{B} a finite number of intersections of \mathcal{B} with a small strip around a resonant plane in \mathbb{R}^{n_1} , assuring that the width of the strip decreases fast enough so that the remaining set always has a non-empty interior part. By the way, this is also strongly reminiscent of the process of construction of a Cantor set. The final goal is to prove that one is left with a Cantor set on non-resonant frequencies which satisfy the required resonance conditions and has positive Lebesgue measure. Moreover, the relative measure with respect to \mathcal{B} tends to one when the size of the perturbation is decreased to zero. This is the underlying idea of the proof that we plan to present in complete form in [17].

Leaving again the proof of the algorithm convergence to a forthcoming paper, we report more precise statements about the previous informal discussion. Let us emphasize that Hamiltonian (9) satisfies the following parity condition: all coefficients of the expansion of $f_{l,m}^{(r,s)}$ having even (odd) trigonometrical degree in the \mathbf{q} variables and odd (even) degree in (\mathbf{x}, \mathbf{y}) , are identically zero. In the planetary case this is a straightforward consequence of d'Alembert rules.

Theorem 3.1 *Consider a set of Hamiltonians parametrized with respect to the frequency $\omega^{(0)}$ that are analytic on some suitable open domain (of their canonical variables) and are of the form (9) with $r = 1$, namely*

$$H^{(0)}(\mathbf{p}, \mathbf{q}, \mathbf{x}, \mathbf{y}; \omega^{(0)}) = \omega^{(0)} \cdot \mathbf{p} + \Omega^{(0)}(\omega^{(0)}) \cdot \mathbf{J} + \sum_{s=0}^{\infty} \sum_{l=0}^{\infty} \sum_{\substack{2j_1+j_2=l \\ j_1 \geq 0, j_2 \geq 0}} f_{j_1, j_2}^{(0,s)}(\mathbf{p}, \mathbf{q}, \mathbf{x}, \mathbf{y}; \omega^{(0)}) .$$

Assume the following hypotheses to be fulfilled:

(i) *let $\omega^{(0)} \mapsto \Omega^{(0)}(\omega^{(0)})$ be a regular function defined on an open set $\mathcal{B} \subset \mathbb{R}^{n_1}$ such that*

$$|\mathbf{l} \cdot \Omega^{(0)}(\omega^{(0)})| \geq \Xi_0 , \quad \forall |\mathbf{l}| = 1, 2, \quad \omega^{(0)} \in \mathcal{B} ,$$

and

$$\|\Omega^{(0)}(\boldsymbol{\omega}^{(0)}) - \Omega^{(0)}(\tilde{\boldsymbol{\omega}}^{(0)})\| \leq L_0 \|\boldsymbol{\omega}^{(0)} - \tilde{\boldsymbol{\omega}}^{(0)}\|, \quad \forall \boldsymbol{\omega}^{(0)}, \tilde{\boldsymbol{\omega}}^{(0)} \in \mathcal{B},$$

for some positive constants Ξ_0 and L_0 ;

(ii) the functions $f_{j_1, j_2}^{(0, s)} \in \mathcal{P}_{j_1, j_2}^{(sK)} \forall j_1, j_2, s \geq 0$ with a fixed integer value of $K > 0$; furthermore, they satisfy the parity condition above and

$$\begin{aligned} f_{0,0}^{(0,0)} = f_{0,1}^{(0,0)} = f_{0,2}^{(0,0)} = f_{1,0}^{(0,0)} &= 0, \\ \langle f_{0,0}^{(0,1)} \rangle_{\mathbf{q}} = \langle f_{0,1}^{(0,1)} \rangle_{\mathbf{q}} = \langle f_{0,2}^{(0,1)} \rangle_{\mathbf{q}} = \langle f_{1,0}^{(0,1)} \rangle_{\mathbf{q}} &= 0; \end{aligned} \quad (38)$$

(iii) the non-degeneracy condition

$$\det \left(\frac{\partial^2 f_{2,0}^{(0,0)}}{\partial p_i \partial p_j} \right)_{i,j=1,\dots,n_1} \neq 0,$$

is satisfied $\forall \boldsymbol{\omega}^{(0)} \in \mathcal{B}$ and \mathbf{p} in the definition domain of the Hamiltonians;

(iv) the following upper bounds hold true:

$$\|f_{j_1, j_2}^{(0, s)}\| \leq \varepsilon^s E, \quad \forall j_1, j_2, s \geq 0, \quad (39)$$

for some positive constants ε and E , with ε small enough.

Then, there exists a Cantor set $\mathcal{S} \subset \mathcal{B}$ of positive Lebesgue measure (in \mathbb{R}^{n_1}), such that for each $\boldsymbol{\omega}^{(0)} \in \mathcal{S}$ there is an analytic canonical transformation giving the Hamiltonian the normal form (8), namely,

$$\begin{aligned} H^{(\infty)}(\mathbf{P}, \mathbf{Q}, \mathbf{X}, \mathbf{Y}; \boldsymbol{\omega}^{(0)}) &= \boldsymbol{\omega}^{(\infty)} \cdot \mathbf{P} + \sum_{j=1}^{n_2} \frac{\Omega_j^{(\infty)} (X_j^2 + Y_j^2)}{2} + \\ &\mathcal{O}(\|\mathbf{P}\|^2) + \mathcal{O}(\|\mathbf{P}\| \|\mathbf{X}, \mathbf{Y}\|) + \mathcal{O}(\|\mathbf{X}, \mathbf{Y}\|^3), \end{aligned}$$

where $\boldsymbol{\omega}^{(\infty)} = \boldsymbol{\omega}^{(\infty)}(\boldsymbol{\omega}^{(0)})$ and $\Omega^{(\infty)} = \Omega^{(\infty)}(\boldsymbol{\omega}^{(0)})$.

In the statement above, the functional norm appearing in (39) is defined as the sum of the absolute values of the coefficients appearing in the Taylor-Fourier expansion of $f_{j_1, j_2}^{(0, s)}$. Let us recall that, as remarked at the beginning of section 3, the n_1 -dimensional (elliptic) torus corresponding to $\mathbf{P} = \mathbf{0}$ and $\mathbf{X} = \mathbf{Y} = \mathbf{0}$ is invariant, and carries quasi periodic orbits with frequencies $\boldsymbol{\omega}^{(\infty)}$. Moreover, let us emphasize that taking control of the measure of the set \mathcal{S} is perhaps the main difficulty of the proof. Indeed, the definition of \mathcal{S} is very delicate, because it is such that $\forall \boldsymbol{\omega}^{(0)} \in \mathcal{S}$ the sequence $\{(\boldsymbol{\omega}^{(r)}, \Omega^{(r)})\}_{r \geq 0}$ (that is introduced by the algorithm described in the present section) starting from $(\boldsymbol{\omega}^{(0)}, \Omega^{(0)}(\boldsymbol{\omega}^{(0)}))$ satisfies the following conditions $\forall r \geq 1$:

$$\min_{\substack{0 < |\mathbf{k}| \leq rK \\ 0 \leq |\mathbf{l}| \leq 2}} |\mathbf{k} \cdot \boldsymbol{\omega}^{(r-1)} + \mathbf{l} \cdot \Omega^{(r-1)}| \geq \frac{\gamma}{(rK)^\tau}, \quad \min_{|\mathbf{l}|=2} |\mathbf{l} \cdot \Omega^{(r-1)}| \geq \beta \quad (40)$$

for some positive fixed values of γ , β and $\tau > n_1 - 1$.

Let us now come to the numerical aspect. At first sight the formal algorithm seems to require a cumbersome trial and error procedure in order to find the good frequencies: when some of the non-resonance conditions fail to be satisfied at a given step, one should change the initial frequencies and restart the whole process. Moreover, since the non-resonance condition must be satisfied by the final frequencies, which obviously can not be calculated, the whole process seems to be unsuitable for a rigorous proof. We explain here in which sense the computer-assisted proofs can help to improve the results also in this context. We make two remarks.

The first remark is connected with the use of interval arithmetic while performing the actual construction. Following the suggestion of the analytic scheme of the proof, we look for uniform estimates on a small open ball \mathcal{B} , such that $\forall \omega^{(0)} \in \mathcal{B}$ we explicitly perform R normalization steps, with R as large as possible. Essentially, we may reproduce numerically the process of eliminating step-by-step the unwanted resonant frequencies by suitably determining the intervals. Once R steps have been explicitly performed, we may apply to the partially normalized Hamiltonian $H^{(R)}$ a suitable formulation of the KAM theorem for elliptic tori. This means that we recover the scheme that we have already applied to the case of maximal dimension tori. That is, we can take advantage of the fact that the perturbing terms are much smaller than the corresponding ones for the initial Hamiltonian $H^{(0)}$; thus, in principle we could ensure that for realistic values of μ the relative measure of the invariant tori is so large that the set of those $\omega^{(0)}$ for which the algorithm can not work (i.e., $\mathcal{B} \setminus \mathcal{S}$) is so small that it can be neglected when we are dealing with a practical application.

The second remark is that we may take a more practical attitude, relying on the fact that the set of good frequencies, according to the theory, has Lebesgue measure close to one, so that the case of frequencies which are resonant at some finite order occurs with very low probability. Thus, we just make a choice of the initial frequencies and proceed with the construction, checking at every order that the non-resonance conditions that we need at that order are fulfilled. We emphasize that the most extended resonant regions are those of low order, so that it is not very difficult to check initially that the chosen frequencies will likely be good enough. It may happen, of course, that the whole procedure must be restarted with different frequencies, but this case is reasonably expected to occur only rarely. For, since the size of the perturbation is expected to decrease geometrically, we may confidently expect that the probability of failure will decrease, too. This is actually confirmed by the calculations we have done.

When R steps have been made, in principle we can apply the theorem to a small neighborhood of the calculated frequencies by choosing a suitable initial ball around the frequencies approximated at that step.

4 Elliptic Tori for the SJSU System

We come now to the application of the formal algorithm for the construction of an elliptic torus to the planar SJSU system. Here we explicitly construct the normal form at a finite

order checking that the norms of the generating functions decrease as predicted by the theory. Then we perform a numerical check by comparing the orbit obtained via the normal form with the numerically integrated one.

The initial Hamiltonian is written in (5), with a suitable rearrangement of terms so that it is given the form (9) with $r = 1$. This requires also a diagonalization of the quadratic part in the secular variables, which is performed as described at the end of sect. 2.

4.1 Constructing the Elliptic Torus by Using Computer Algebra

We applied the algorithm constructing elliptic tori (which has been widely described in sect. 3) to the Hamiltonian $H^{(0)}$ (that is defined in (6) and has been obtained as described in sect. 2). The parameters have been fixed according to the specific values of the planar SJSU system, which are reported in table 1. Our software package for computer algebra allowed us to explicitly calculate all the expansions (6) of $H^{(r)}$ with index r ranging between 0 and 9, so to include: (c1) the terms having degree j_1 in the actions \mathbf{p} with $j_1 \leq 3$, (c2) all terms having degree j_2 in the variables (\mathbf{x}, \mathbf{y}) , with j_2 such that $2j_1 + j_2 \leq 8$, (c3) all terms up to the trigonometric degree 18 with respect to the angles \mathbf{q} . The truncation rules (c1)–(c3) are in agreement with those prescribed about the expansion (5) in sect. 2 at points (b1)–(b3). Let us remark that both the truncation rules (c1) and (c2) are preserved by all canonical transformations included in our algorithm. Moreover, we have found that fixing $K = 2$ is a suitable choice to have a rather regular decreasing of the size of the generating functions when the normalization step r is increased, as shown in fig. 1. Since the maximal trigonometric degree of the generating functions $\chi_0^{(r)}$, $\chi_1^{(r)}$, $X_2^{(r)}$ and $Y_2^{(r)}$ is equal to rK , the choice to set $K = 2$ and the rule (c3) explain why we stopped the algorithm after having ended the normalization step with $r = 9$.

The behavior of the norms of the generating functions is reported in fig. 1. Let us make a few comments. The theoretical estimates assure the convergence of the normal form provided the norms decrease geometrically with the order. The figure shows that this is indeed the behavior in our case. The behavior of the $\mathcal{D}_2^{(r)}$ functions appears to be quite irregular, but we should recall that these functions do not play the role of *normalization* function, since they represent the *diagonalization* of the quadratic part related to the secular variables. We emphasize that the presence of a dangerous resonance would be reflected in a sudden increase of the coefficients; thus, the plot may be considered as a practical confirmation that the frequencies are well chosen.

Concerning the computational effort, performing the construction of the normal form up to order $r = 9$ has taken about 10 hours of CPU time on an Intel Core i7, using about 6 Gb of RAM.

4.2 Explicit Calculation of the Orbits on the Elliptic Torus

We now perform a check on the approximation of the elliptic torus. To this end, we calculate the orbit on the torus using the analytic expression and we compare it with

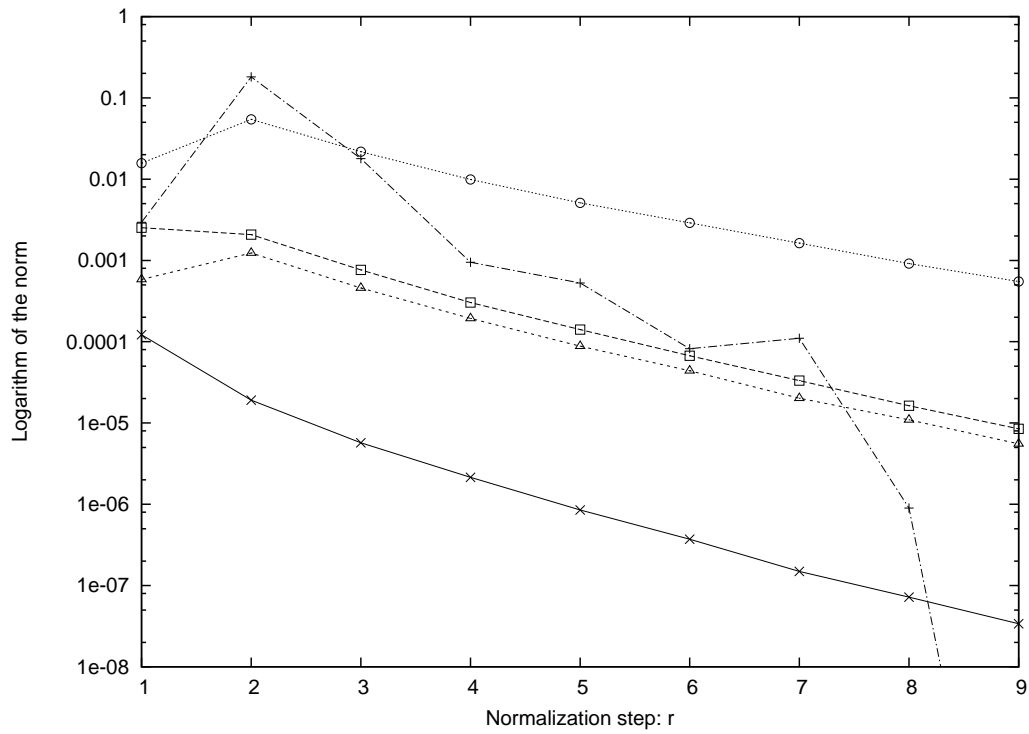


Figure 1: Numerical check of the algorithm constructing the normal form related to an elliptic torus for the planar SJSU system: plot of the norm of the generating functions as a function of the normalization step r ; more precisely, the symbols \times , \square , \triangle , \circ and $+$ refer to the norm of the generating functions $\chi_0^{(r)}$, $\chi_1^{(r)}$, $X_2^{(r)}$, $Y_2^{(r)}$ and $\mathcal{D}_2^{(r)}$, respectively, which are defined during the normalization algorithm, as described in sect. 3. The norm is calculated by adding up the absolute values of all coefficients appearing in the expansion of each generating function.

a numerical integration of Hamilton's equations. In this subsection we explain how the calculation of the orbit via normal form is performed.

According to the theory of Lie series, the canonical transformation $(\mathbf{p}, \mathbf{q}, \mathbf{x}, \mathbf{y}) = \mathcal{K}^{(r)}(\mathbf{p}^{(r)}, \mathbf{q}^{(r)}, \mathbf{x}^{(r)}, \mathbf{y}^{(r)})$ inducing the normalization up to the step r is given by

$$\begin{aligned} \mathcal{K}^{(r)}(\mathbf{p}^{(r)}, \mathbf{q}^{(r)}, \mathbf{x}^{(r)}, \mathbf{y}^{(r)}) &= \exp \mathcal{L}_{\mathcal{D}_2^{(r)}} \circ \exp \mathcal{L}_{Y_2^{(r)}} \circ \exp \mathcal{L}_{X_2^{(r)}} \circ \\ &\quad \exp \mathcal{L}_{X_1^{(r)}} \circ \exp \mathcal{L}_{X_0^{(r)}} \circ \dots \circ \exp \mathcal{L}_{\mathcal{D}_2^{(1)}} \circ \exp \mathcal{L}_{Y_2^{(1)}} \circ \\ &\quad \exp \mathcal{L}_{X_2^{(1)}} \circ \exp \mathcal{L}_{X_1^{(1)}} \circ \exp \mathcal{L}_{X_0^{(1)}} (\mathbf{p}^{(r)}, \mathbf{q}^{(r)}, \mathbf{x}^{(r)}, \mathbf{y}^{(r)}), \end{aligned} \quad (41)$$

where $(\mathbf{p}^{(r)}, \mathbf{q}^{(r)}, \mathbf{x}^{(r)}, \mathbf{y}^{(r)})$ are meant to be the new coordinates. Thus, the canonical transformation $(\mathbf{p}, \mathbf{q}, \mathbf{x}, \mathbf{y}) = \mathcal{K}^{(\infty)}(\mathbf{P}, \mathbf{Q}, \mathbf{X}, \mathbf{Y})$ brings the initial Hamiltonian $H^{(0)}$ in the normal form $H^{(\infty)} = H^{(0)} \circ \mathcal{K}^{(\infty)}$, which is written in (7), with $\mathcal{K}^{(\infty)} = \lim_{r \rightarrow \infty} \mathcal{K}^{(r)}$. Let us introduce a new symbol to denote the composition of all the canonical changes of coordinates defined in sects. 2 and 3, i.e.,

$$\mathcal{C}^{(r)} = \mathcal{E} \circ \mathcal{T}_{\Lambda^*} \circ \mathcal{D} \circ \mathcal{K}^{(r)}, \quad (42)$$

where $(\tilde{\mathbf{r}}, \mathbf{r}) = \mathcal{E}(\Lambda, \boldsymbol{\lambda}, \boldsymbol{\xi}, \boldsymbol{\eta})$ is the canonical transformation giving the heliocentric positions \mathbf{r} and their conjugated momenta $\tilde{\mathbf{r}}$ as a function of the Poincaré's variables. If $(\tilde{\mathbf{r}}(0), \mathbf{r}(0))$ is an initial condition on an invariant elliptic torus, in principle we might use the following calculation scheme to integrate the equation of motion:

$$\begin{array}{ccc} (\tilde{\mathbf{r}}(0), \mathbf{r}(0)) & \xrightarrow{(\mathcal{C}^{(\infty)})^{-1}} & (\mathbf{P}(0) = \mathbf{0}, \mathbf{Q}(0), \mathbf{X}(0) = \mathbf{0}, \mathbf{Y}(0) = \mathbf{0}) \\ & & \downarrow \Phi_{\boldsymbol{\omega}^{(\infty)}, \mathbf{P}}^t \\ (\tilde{\mathbf{r}}(t), \mathbf{r}(t)) & \xleftarrow{\mathcal{C}^{(\infty)}} & (\mathbf{P}(t) = \mathbf{0}, \mathbf{Q}(t) = \mathbf{Q}(0) + \boldsymbol{\omega}^{(\infty)}t, \mathbf{X}(t) = \mathbf{0}, \mathbf{Y}(t) = \mathbf{0}) \end{array}, \quad (43)$$

where $\Phi_{\boldsymbol{\omega}^{(\infty)}, \mathbf{P}}^t$ induces the quasi-periodic flow related to the frequencies vector $\boldsymbol{\omega}^{(\infty)}$. Of course, the previous scheme requires an unlimited computing power; from a practical point of view, we can just approximate it by replacing $\mathcal{C}^{(\infty)}$ with $\mathcal{C}^{(R)}$, being R as large as possible. Thus, the integration via normal form actually reduces to a transformation of the coordinates of the initial point to the coordinates of the normal form, the calculation of the flow at time t in the latter coordinates, which is a trivial matter since the flow is exactly quasi-periodic with known frequencies, followed by a transformation back to the original coordinates.

The rough but natural check that one can perform consists precisely in comparing the orbit calculated via the semi-analytic scheme just described with the result of a direct numerical integration. As it has been shown in [35], [36], [37] and [11], this kind of comparisons provide a very stressing test for the accuracy of the whole algorithm constructing the normal form.

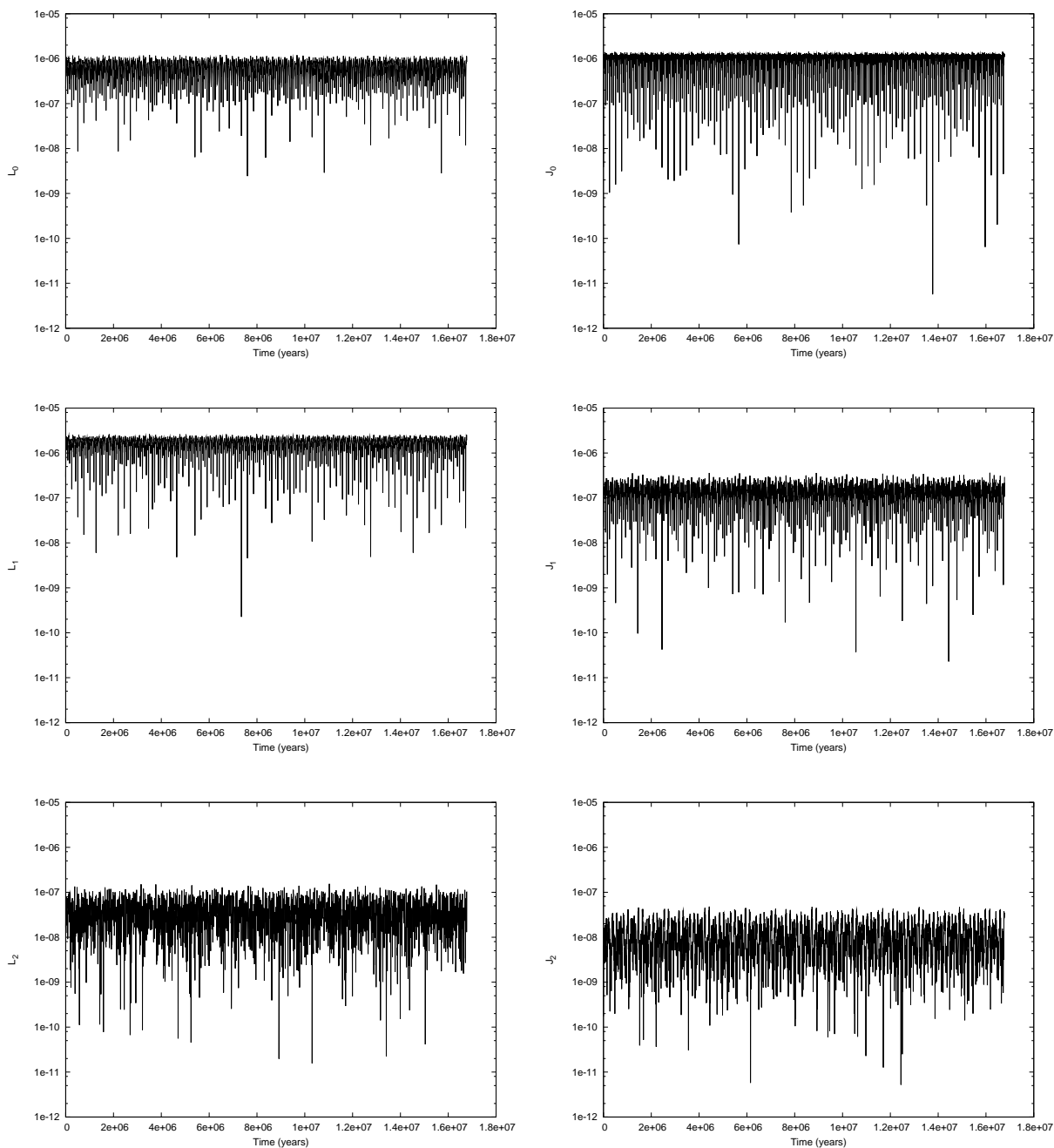


Figure 2: Time evolution of the normalized fast actions p_1, p_2, p_3 and of the slow actions J_1, J_2, J_3 along a numerically integrated orbit. These quantities should be zero on the elliptic torus, and one sees here that they take indeed very small values along the orbit, thus showing that the approximation of the elliptic torus is good enough.

The initial condition $(\tilde{\mathbf{r}}(0), \mathbf{r}(0))$ of the orbit that we want to study is not directly provided by the observations. Thus, here we perform a test in a slightly different way with respect to previous papers. Precisely, we check that the normalized variables \mathbf{P} , \mathbf{X} and \mathbf{Y} remain constantly equal to zero along the motion on an elliptic torus. Let p_1, p_2, p_3 and J_1, J_2, J_3 denote the fast actions and the secular actions of the Hamiltonian normalized up to order R (we omit the upper index R for simplicity). Setting $p_1(0) = p_2(0) = p_3(0) = 0$ and $J_1(0) = J_2(0) = J_3(0) = 0$ we have a point on the elliptic torus, and by applying the transformations we get the initial condition $(\tilde{\mathbf{r}}(0), \mathbf{r}(0))$. More precisely, we focus on the case $R = 9$ and we consider the initial conditions

$$(\mathcal{C}^{(9)}) (\mathbf{0}, \mathbf{0}, \mathbf{0}, \mathbf{0}) ; \quad (44)$$

according to the calculation method described in this section. This should be an accurate approximation of a point on an elliptic torus. Therefore, we preliminarily integrated the motion of the planar SJSU system over a time interval of 2^{24} years, by using the symplectic method \mathcal{SBAB}_3 (see [33]) with a time-step of 0.04 years. For a set of points on the orbit we apply the canonical transformation $(\mathcal{C}^{(9)})^{-1}$, and so we calculate the evolved actions $p_1(t), p_2(t), p_3(t)$ and $J_1(t), J_2(t), J_3(t)$, which should be zero for all t apart from a small oscillation due to the approximation of the invariant torus. The results are illustrated in fig. 2, where it is seen that the value of the actions remains very small, reaching about 10^{-6} in the worst cases.

4.3 Validation of the Results by Using Frequency Analysis

Another more refined test is based on frequency map analysis (see, e.g., [31] and [32] for an introduction). The key point is that, according to the ideal calculation scheme (43), the time evolution of every pair of canonical coordinates (e.g. the maps $t \mapsto \tilde{r}_l(t) + ir_l(t)$ with $l = 1, 2, 3$) may be expressed as

$$\sum_{j=0}^{\infty} c_j \exp(i\zeta_j t), \quad \text{where, } \forall j \geq 0, \quad c_j \in \mathbb{C} \text{ and } \exists \mathbf{k}_j \in \mathbb{Z}^{n_1} \text{ such that } \zeta_j = \mathbf{k}_j \cdot \boldsymbol{\omega}^{(\infty)}. \quad (45)$$

Thus, the frequency spectrum is a very peculiar one, since it contains only combinations of the fast frequencies, while no secular frequencies should appear. By the way, the same peculiarity of the spectrum is characteristic of any signal produced by calculating the evolution of a pair of mechanical quantities along an orbit on the elliptic torus. This is what we want to check in the present section. From a strictly mathematical point of view, let us recall that the previous formula for the Fourier spectrum can be deduced by the scheme (43), because the conjugacy function $\mathbf{Q} \mapsto \mathcal{C}^{(\infty)}(\mathbf{0}, \mathbf{Q}, \mathbf{0}, \mathbf{0})$ is analytic, as follows from the convergence of the constructive algorithm that we shall prove in a forthcoming paper.

The orbit with initial point as in the previous sect. 4.2 has been sampled with a time interval of 1 year.⁴ The fast frequencies $\boldsymbol{\omega}^{(\infty)}$ have been accurately determined by

⁴Here we should add a remark concerning the precision of the calculation. In order to have a signal

looking at the main components of the Fourier spectrum of the signals $\Lambda_l(t) \exp(i\lambda_l(t))$, with $l = 1, 2, 3$. As test functions we used the time evolution of the secular Poincaré's variables, namely $\xi_l(t) + i\eta_l(t)$ with $l = 1, 2, 3$. The corresponding signals have been submitted to the frequency analysis method using the so-called Hanning filter. The reason for the choice of the coordinates as test functions is that if the initial point given by (43) is not on the elliptic invariant torus then the presence of secular frequencies is expected to be particularly evident in these signals.

In table 2 we report our numerical results about the first 25 terms of the decomposition (45) for the Uranus secular signal, i.e., $\xi_3(t) + i\eta_3(t)$. The vectors $\mathbf{k}_j \in \mathbb{Z}^{n_1}$ listed in the third column are determined so that the absolute difference $|\zeta_j - \mathbf{k}_j \cdot \boldsymbol{\omega}^{(\infty)}|$ is minimized, with the limit $|\mathbf{k}_j| \leq 20$. We stress that some limits on the absolute value of \mathbf{k}_j must be imposed in order to make consistent its calculation, and our choice is motivated by the fact that the decay of Fourier coefficients in the analytic conjugacy function $\mathcal{C}^{(\infty)}(\mathbf{0}, \mathbf{Q}, \mathbf{0}, \mathbf{0})$ leads us to expect that the main contributions to the spectrum are related to low order harmonics.

If the initial conditions (44) were exactly on an elliptic torus, each value $|\zeta_j - \mathbf{k}_j \cdot \boldsymbol{\omega}^{(\infty)}|$ reported in the fourth column of table 2 should be equal to zero. We see that all of them, except for the cases corresponding to $j = 16, 24$, are actually small enough to be considered as generated by round-off errors. On the other hand, we can definitely say that $\zeta_{16} \simeq -1.1 \times 10^{-5}$ and $\zeta_{24} \simeq -1.9 \times 10^{-5}$ are "secular frequencies", because their values are $\mathcal{O}(\mu)$. Indeed, let us recall that $\mu \simeq 10^{-3}$, but the mass ratio for Uranus, i.e., $m_3/m_0 \simeq 4.4 \times 10^{-5}$, is even smaller.

Let us say that a total absence of secular frequencies can occur only in a very ideal situation, namely: (i) all the calculations described in sects. 2 and 3 should be carried out without performing any truncations on the expansions, (ii) the initial conditions (44) should be replaced with $\mathcal{C}^{(\infty)}(\mathbf{0}, \mathbf{0}, \mathbf{0}, \mathbf{0})$, (iii) no numerical errors should be there. Concerning the point (iii), the numerical error does clearly appear in our signal, but it turns out to be very small. The points (i) and (ii) are more relevant, because our analytical calculation gives a point close to, but not lying on the elliptic torus. Thus the presence of secular frequencies should be expected, and the size of the corresponding coefficients may be considered as a measure of the distance of the initial point from the invariant torus. Nevertheless, it is very remarkable that the amplitude of the first found secular frequency, i.e., $|c_{16}|$, is three orders of magnitude smaller than the main component of the spectrum. We consider this fact as a clear indication that our algorithm is able to identify the elliptic torus with a remarkable precision.

Other components corresponding to secular frequencies are expected to be even smaller than those found with $j = 16, 24$. In fact, let us recall that the frequency analysis method detects the summands $c_j \exp(i\zeta_j t)$ appearing in (45) in a nearly decreasing order with respect to the amplitude $|c_j|$ (for instance, just two exchanges are needed in order to rewrite table 2 in the correct decreasing order); moreover, we calculated that the

clean enough to be analyzed a particular care about the precision is mandatory. After some trials tuning the parameters of the numerical integration, we found that the 80 bits floating point numbers provided by the current AMD and INTEL CPUs fits our needs. Technically this is obtained by using the `long double` types of the GNU C compiler under a Linux operating system.

Table 2: Decomposition of the Fourier spectrum of the signal $\xi_3(t) + i\eta_3(t)$, which is related to the Uranus secular motion. The numerical values in the table have been obtained by applying the frequency analysis method. See the text for more details.

j	ζ_j	\mathbf{k}_j	$ \zeta_j - \mathbf{k}_j \cdot \boldsymbol{\omega}^{(\infty)} $	$ c_j $
0	$-7.48019221455542005 \times 10^{-2}$	(0, 0, -1)	$0.0 \times 10^{+00}$	2.9770×10^{-4}
1	$3.80127210702886631 \times 10^{-1}$	(1, 0, -2)	5.6×10^{-17}	5.5428×10^{-5}
2	$6.37064849761184715 \times 10^{-2}$	(0, 1, -2)	5.6×10^{-17}	1.8199×10^{-5}
3	$2.02214892097791255 \times 10^{-1}$	(0, 2, -3)	$0.0 \times 10^{+00}$	1.7410×10^{-5}
4	$3.40723299219463982 \times 10^{-1}$	(0, 3, -4)	$0.0 \times 10^{+00}$	6.1013×10^{-6}
5	$8.35056343551327518 \times 10^{-1}$	(2, 0, -3)	5.6×10^{-17}	3.7452×10^{-6}
6	$4.79231706341136876 \times 10^{-1}$	(0, 4, -5)	1.7×10^{-16}	2.4485×10^{-6}
7	$-2.13310329267227178 \times 10^{-1}$	(0, -1, 0)	2.5×10^{-16}	1.4521×10^{-6}
8	$-3.51818736388899878 \times 10^{-1}$	(0, -2, 1)	2.2×10^{-16}	1.0175×10^{-6}
9	$6.17740113462809326 \times 10^{-1}$	(0, 5, -6)	1.1×10^{-16}	1.0447×10^{-6}
10	$1.28998547639976824 \times 10^{+0}$	(3, 0, -4)	2.2×10^{-16}	7.8098×10^{-7}
11	$-4.90327143510572494 \times 10^{-1}$	(0, -3, 2)	1.1×10^{-16}	7.1175×10^{-7}
12	$7.56248520584482442 \times 10^{-1}$	(0, 6, -7)	2.2×10^{-16}	4.6141×10^{-7}
13	$-9.84660187842435808 \times 10^{-1}$	(-2, 0, 1)	1.7×10^{-16}	4.1885×10^{-7}
14	$-6.28835550632244611 \times 10^{-1}$	(0, -4, 3)	5.0×10^{-16}	3.8157×10^{-7}
15	$-5.29731054993994532 \times 10^{-1}$	(-1, 0, 0)	5.6×10^{-16}	2.9840×10^{-7}
16	$-1.11363990387936461 \times 10^{-5}$	(0, 0, 0)	1.1×10^{-05}	2.2654×10^{-7}
17	$8.94756927706155003 \times 10^{-1}$	(0, 7, -8)	1.1×10^{-16}	2.0832×10^{-7}
18	$-7.67343957753918837 \times 10^{-1}$	(0, -5, 4)	1.0×10^{-15}	1.9160×10^{-7}
19	$1.74491460924820907 \times 10^{+0}$	(4, 0, -5)	2.8×10^{-16}	1.7777×10^{-7}
20	$-1.43958932069087675 \times 10^{+0}$	(-3, 0, 2)	1.1×10^{-16}	1.3450×10^{-7}
21	$2.43025734926846093 \times 10^{-2}$	(-1, 4, -4)	1.1×10^{-14}	1.1086×10^{-7}
22	$-9.05852364875589622 \times 10^{-1}$	(0, -6, 5)	9.4×10^{-16}	9.3984×10^{-8}
23	$1.03326533482782756 \times 10^{+0}$	(0, 8, -9)	$0.0 \times 10^{+00}$	9.5496×10^{-8}
24	$-1.96924221667578817 \times 10^{-5}$	(0, 0, 0)	2.0×10^{-05}	5.2900×10^{-8}

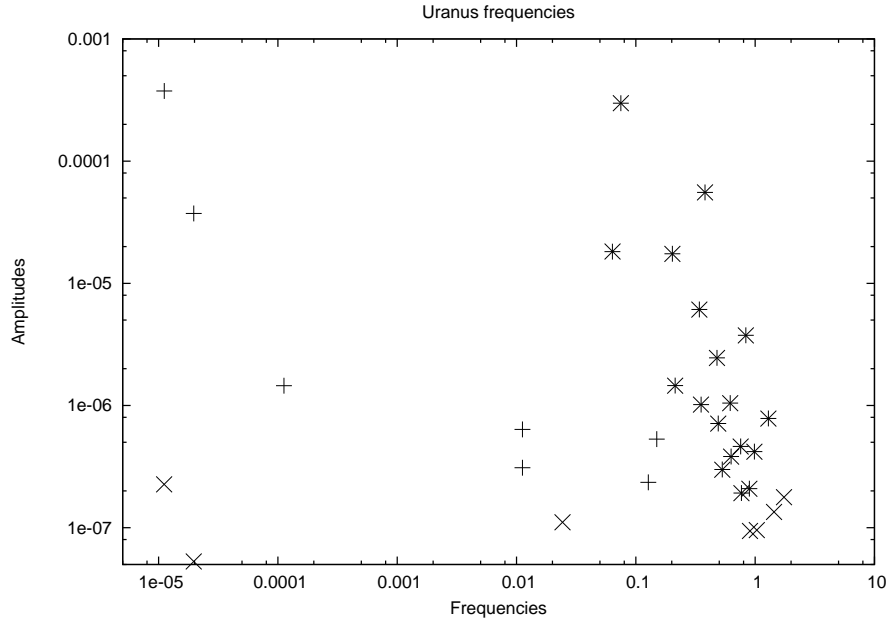


Figure 3: Frequency analysis of the secular signal related to the secular Uranus motion: $\xi_3(t) + i\eta_3(t) = \sum_{j=0}^{\infty} c_j \exp(i\zeta_j t)$. Plot of the amplitudes $|c_j|$ as a function of the frequencies ζ_j in Log-Log scale. The symbol \times [$+$, resp.] refer to the signal related to the motion starting from the initial conditions (44) [(46), resp.], i.e., the approximation of a point on an elliptic torus after having performed 9 [0, resp.] steps of the algorithm constructing the corresponding normal form. In both cases, the results for just the first 25 components have been reported in the figure above.

discrepancy $|\xi_3(t) + i\eta_3(t) - \sum_{j=0}^{24} c_j \exp(i\zeta_j t)|$ is smaller than about $\simeq 3.7 \times 10^{-7}$ for all the time values t for which we sampled the signal. Let us emphasize that such an upper bound on the maximal discrepancy is just a little larger than the amplitude $|c_{16}|$.

A similar decomposition has been calculated for both the signals $\xi_1(t) + i\eta_1(t)$ and $\xi_2(t) + i\eta_2(t)$ (which are related to the secular motions of Jupiter and Saturn, respectively). The behavior is very similar to that of table 2, so we omit the corresponding tables.

In order to check the effectiveness of our algorithm, let us further investigate the results as a function of the normalization step in a few different ways.

First, in fig. 3 we plot the amplitudes $|c_j|$ as a function of the frequencies ζ_j in Log-Log scale. We compare the amplitudes corresponding to two different orbits, namely: (a) the orbit with initial point calculated as in (44), and (b) the orbit with initial point

$$\mathcal{C}^{(0)}(\mathbf{0}, \mathbf{0}, \mathbf{0}, \mathbf{0}). \quad (46)$$

The symbol \times and $+$ correspond to the orbits (a) and (b), respectively. So the data marked with \times refer to the decomposition of table 2. Let us remark that $\mathcal{C}^{(0)}(\mathbf{0}, \mathbf{0}, \mathbf{0}, \mathbf{0}) = \mathcal{E} \circ \mathcal{T}_{\Lambda^*} \circ \mathcal{D}(\mathbf{0}, \mathbf{0}, \mathbf{0}, \mathbf{0})$ is a sort of trivial approximation of a point on the elliptic torus as it is provided by simply avoiding to apply the part of our algorithm constructing the normal form, as it is described in sect. 3. Let us recall that the amplitudes related to

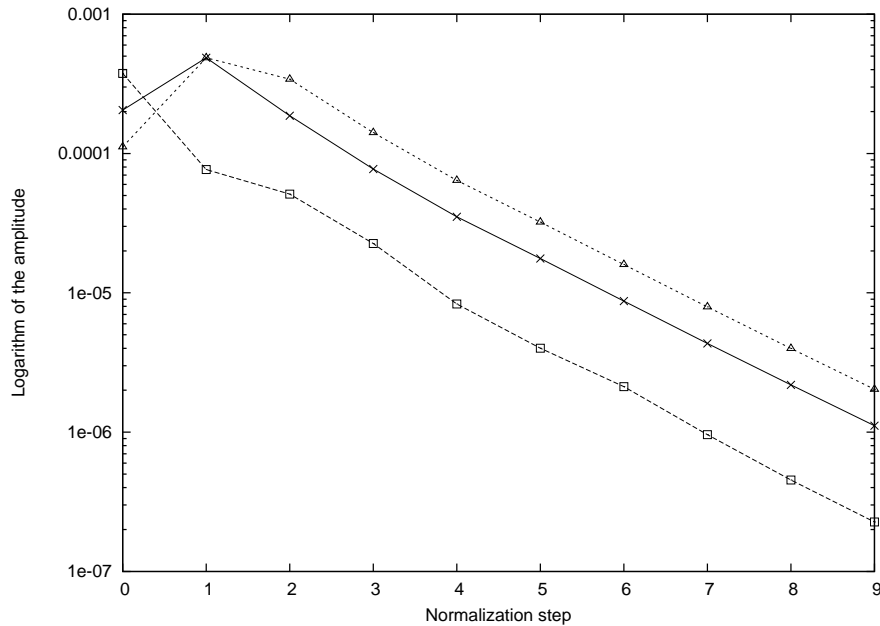


Figure 4: Frequency analysis of the signal related to the secular motion of Jupiter, Saturn and Uranus, i.e., $\xi(t) + i\eta(t) = \sum_{j=0}^{\infty} c_j \exp(i\zeta_j t)$, where ξ and η are the secular Poincaré variables of a planet (recall definition (2)). Plot of the logarithm of the amplitude $|c_j|$ related to the main secular component as a function of the normalization step. The symbols \times , Δ and \square refer to signals corresponding to Jupiter, Saturn and Uranus, respectively.

secular frequencies are expected to have a size $\mathcal{O}(\mu)$. Thus, they are easily separated from the fast ones, having a size less than 10^{-3} . By looking at the right side of fig. 3, one immediately sees that the part of the spectrum related to the fast frequencies is nearly indistinguishable when the initial conditions (44) or (46) are considered, because the symbols \times and $+$ superpose each other almost exactly for most of the main components. On the other hand, the secular part of the spectrum, that is in the left side of fig. 3, strongly differs. In fact, when the initial conditions (46) (that trivially approximate a point on the elliptic torus) are considered, three secular frequencies are detected; while just two of them are found in the case of the more accurate initial data (44). Moreover, by comparing the amplitudes, one can see that the better approximation of the torus with the orbit (a) makes the corresponding secular amplitudes (\times) to be approximately three orders of magnitude smaller than the amplitudes ($+$) for orbit (b). The results are very similar for the three planets, thus we reported only those for Uranus.

For completeness we report in fig. 4 the amplitude of the main secular component of the signals for the three planets as a function of the normalization step. The symbols \times , Δ and \square refer to the data for Jupiter, Saturn and Uranus, respectively. A sharp geometric decay to zero is observed, which makes evident the effectiveness of our procedure constructing the normal form for an elliptic torus.

Finally, it is interesting to look at the change of the secular frequencies during the

Table 3: Values of the frequencies $\Omega^{(r)}$ of the transversal oscillation with respect to the elliptic torus.

Step (r)	$\Omega_0^{(r)}$	$\Omega_1^{(r)}$	$\Omega_2^{(r)}$
0	$-1.0779281 \times 10^{-4}$	$-1.7700018 \times 10^{-5}$	$-1.1005216 \times 10^{-5}$
1	$-1.0837401 \times 10^{-4}$	$-1.7718250 \times 10^{-5}$	$-1.0998189 \times 10^{-5}$
2	$-1.1413488 \times 10^{-4}$	$-1.9540195 \times 10^{-5}$	$-1.1137012 \times 10^{-5}$
3	$-1.1211306 \times 10^{-4}$	$-1.9684669 \times 10^{-5}$	$-1.1133050 \times 10^{-5}$
4	$-1.1207431 \times 10^{-4}$	$-1.9686809 \times 10^{-5}$	$-1.1133969 \times 10^{-5}$
5	$-1.1207181 \times 10^{-4}$	$-1.9691417 \times 10^{-5}$	$-1.1135412 \times 10^{-5}$
6	$-1.1206555 \times 10^{-4}$	$-1.9691851 \times 10^{-5}$	$-1.1135625 \times 10^{-5}$
7	$-1.1206559 \times 10^{-4}$	$-1.9691857 \times 10^{-5}$	$-1.1135808 \times 10^{-5}$
8	$-1.1206555 \times 10^{-4}$	$-1.9691864 \times 10^{-5}$	$-1.1135815 \times 10^{-5}$
9	$-1.1206555 \times 10^{-4}$	$-1.9691864 \times 10^{-5}$	$-1.1135815 \times 10^{-5}$

normalization procedure. The values of the secular frequencies $\Omega^{(r)}$ in (33) of the three planets, calculated at every step of the normalization procedure are collected in the table 3. At step 0 the frequencies so obtained correspond to those given by Lagrange-Laplace theory for our planar model including Sun, Jupiter, Saturn and Uranus. After the first few steps a steady convergence to a final value is highlighted.

Acknowledgments

The authors have been supported by the research program “Dynamical Systems and applications”, PRIN 2007B3RB EY, financed by MIUR. M.S. has been partially supported also by the research program “Studi di Esplorazione del Sistema Solare”, financed by ASI.

References

- [1] V.I. Arnold: *Proof of a theorem of A. N. Kolmogorov on the invariance of quasi-periodic motions under small perturbations of the Hamiltonian*, Usp. Mat. Nauk, **18**, 13 (1963); Russ. Math. Surv., **18**, 9 (1963).
- [2] V.I. Arnold: *Small denominators and problems of stability of motion in classical and celestial mechanics*, Usp. Math. Nauk **18** N.6, 91 (1963); Russ. Math. Surv. **18** N.6, 85 (1963).
- [3] G. Benettin, L. Galgani, A. Giorgilli and J.M. Strelcyn: *A Proof of Kolmogorov’s Theorem on Invariant Tori Using Canonical Transformations Defined by the Lie method*, Nuovo Cimento, **79**, 201–223 (1984).

- [4] L. Biasco, L. Chierchia and E. Valdinoci: *Elliptic two-dimensional invariant tori for the planetary three-body problem*, Arch. Rational Mech. Anal., **170**, 91–135 (2003).
- [5] L. Biasco, L. Chierchia and E. Valdinoci: *N-dimensional elliptic invariant tori for the planar (N+1)-body problem*, SIAM Journal on Mathematical Analysis, **37**, n. 5, 1560–1588 (2006).
- [6] G.D. Birkhoff: *Dynamical systems*, New York (1927).
- [7] A. Celletti, A. Giorgilli and U. Locatelli: *Improved Estimates on the Existence of Invariant Tori for Hamiltonian Systems*, Nonlinearity, **13**, 397–412 (2000).
- [8] E. Castellà and A. Jorba: *On the vertical families of two-dimensional tori near the triangular points of the Bicircular problem*, Cel. Mech. & Dyn. Astr., **76**, 35–54 (2000).
- [9] A. Deprit: *Elimination of the nodes in problems of n bodies*, Cel. Mech. & Dyn. Astr., **30**, 181–195 (1983).
- [10] F. Gabern and A. Jorba: *A restricted four-body model for the dynamics near the Lagrangian points of the Sun–Jupiter system*, DCDS-B, **1**, 143–182 (2001).
- [11] F. Gabern, A. Jorba and U. Locatelli: *On the construction of the Kolmogorov normal form for the Trojan asteroids*, Nonlinearity, **18**, n.4, 1705–1734 (2005).
- [12] A. Giorgilli: *Quantitative methods in classical perturbation theory*, proceedings of the Nato ASI school “From Newton to chaos: modern techniques for understanding and coping with chaos in N-body dynamical systems”, A.E. Roy e B.D. Steves eds., Plenum Press, New York (1995).
- [13] A. Giorgilli and U. Locatelli: *Kolmogorov theorem and classical perturbation theory*, J. of App. Math. and Phys. (ZAMP), **48**, 220–261 (1997).
- [14] A. Giorgilli and U. Locatelli: *On classical series expansion for quasi-periodic motions*, MPEJ, **3**, 5, 1–25 (1997).
- [15] A. Giorgilli, U. Locatelli and M. Sansottera: *Kolmogorov and Nekhoroshev theory for the problem of three bodies*, Cel. Mech. & Dyn. Astr., **104**, 159–173 (2009).
- [16] A. Giorgilli, U. Locatelli and M. Sansottera: *Su un’estensione della teoria di Lagrange per i moti secolari*, Istituto Lombardo (Rend. Scienze), **143**, 223–240 (2009).
- [17] A. Giorgilli, U. Locatelli and M. Sansottera: *A constructive algorithm of the normal form for lower dimensional elliptic tori.*, in preparation.
- [18] W.H. Jefferys and J. Moser: *Quasi-periodic solutions for the three-body problem*, Astronom. J., **71**, 568–578 (1966).

- [19] A. Jorba and J. Villanueva: *On the persistence of lower dimensional invariant tori under quasiperiodic perturbations*, J. of Nonlin. Sci., **7**, 427–473 (1997).
- [20] A. Jorba and J. Villanueva: *On the Normal Behaviour of Partially Elliptic Lower Dimensional Tori of Hamiltonian Systems*, Nonlinearity, **10**, 783–822 (1997).
- [21] A. Jorba and J. Villanueva: *Numerical Computation of Normal Forms Around Some Periodic Orbits of the Restricted Three Body Problem*, Physica D, **114**, 197–229 (1998).
- [22] A.N. Kolmogorov: *Preservation of conditionally periodic movements with small change in the Hamilton function*, Dokl. Akad. Nauk SSSR, **98**, 527 (1954). Engl. transl. in: Los Alamos Scientific Laboratory translation LA-TR-71-67; reprinted in: Lecture Notes in Physics **93**.
- [23] J.L. Lagrange: *Sur l'altération des moyens mouvements des planètes*, Mem. Acad. Sci. Berlin **199** (1776); *Oeuvres complètes*, **VI**, 255, Paris, Gauthier–Villars (1869).
- [24] J.L. Lagrange: *Théorie des variations séculaires des éléments des planètes. Première partie contenant les principes et les formules générales pour déterminer ces variations*, Nouveaux mémoires de l'Académie des Sciences et Belles-Lettres de Berlin (1781); *Oeuvres complètes*, **V**, 125–207, Paris, Gauthier–Villars (1870).
- [25] J.L. Lagrange: *Théorie des variations séculaires des éléments des planètes. Seconde partie contenant la détermination de ces variations pour chacune des planètes principales*, Nouveaux mémoires de l'Académie des Sciences et Belles-Lettres de Berlin (1782); *Oeuvres complètes*, **V**, 211–489, Paris, Gauthier–Villars (1870).
- [26] P.S. Laplace: *Mémoire sur les solutions particulières des équations différentielles et sur les inégalités séculaires des planètes* (1772); *Oeuvres complètes*, **IX**, 325, Paris, Gauthier-Villars (1895).
- [27] P.S. Laplace: *Mémoire sur les inégalités séculaires des planètes et des satellites*, Mem. Acad. royale des Sci. de Paris (1784); *Oeuvres complètes*, **XI**, 49, Paris, Gauthier-Villars (1895).
- [28] P.S. Laplace: *Théorie de Jupiter et de Saturne*, Mem. Acad. royale des Sci. de Paris (1785); *Oeuvres complètes*, **XI**, 164, Paris, Gauthier-Villars (1895).
- [29] J. Laskar: *Systèmes de variables et éléments*, in Benest, D. and Froeschlé, C. (eds.): *Les Méthodes modernes de la Mécanique Céleste*, 63–87, Editions Frontières (1989).
- [30] J. Laskar and P. Robutel: *Stability of the Planetary Three-Body Problem — I. Expansion of the Planetary Hamiltonian*, Celestial Mechanics and Dynamical Astronomy, **62**, 193–217 (1995).
- [31] J. Laskar: *Introduction to frequency map analysis*, in C. Simò (managing ed.), Proceedings of the NATO ASI school: “Hamiltonian Systems with Three or More Degrees of Freedom”, S’Agaró (Spain), June 19–30, 1995, Kluwer, 134–150 (1999).

- [32] J. Laskar: *Frequency Map analysis and quasi periodic decompositions*, in Benest et al. (managing eds): “Hamiltonian systems and Fourier analysis”, Taylor and Francis (2005).
- [33] J. Laskar and P. Robutel: *High order symplectic integrators for perturbed Hamiltonian systems*, *Celestial Mechanics and Dynamical Astronomy*, **80**, 39–62 (2001).
- [34] B. Lieberman: *Existence of quasi-periodic solutions to the three-body problem*, *Cel. Mech. & Dyn. Astr.*, **3**, 408–426 (1971).
- [35] U. Locatelli and A. Giorgilli: *Invariant tori in the secular motions of the three-body planetary systems*, *Cel. Mech. & Dyn. Astr.*, **78**, 47–74 (2000).
- [36] U. Locatelli and A. Giorgilli: *Construction of the Kolmogorov’s normal form for a planetary system*, *Regular and Chaotic Dynamics*, **10**, n.2, 153–171 (2005).
- [37] U. Locatelli and A. Giorgilli: *Invariant tori in the Sun–Jupiter–Saturn system*, *DCDS-B*, **7**, 377–398 (2007).
- [38] F. Malige, P. Robutel and J. Laskar: *Partial reduction in the N-body planetary problem using the angular momentum integral*, *Celestial Mechanics and Dynamical Astronomy*, **84**, 283–316 (2002).
- [39] J. Moser: *On invariant curves of area-preserving mappings of an annulus*, *Nachr. Akad. Wiss. Gött., II Math. Phys. Kl* 1962, 1–20 (1962).
- [40] G. Pinzari: *On the Kolmogorov set for many-body problems*, Ph.D. thesis, Università di Roma Tre (2009); publicly available at the web page: <http://ricerca.mat.uniroma3.it/dottorato/Tesi/pinzari.pdf>.
- [41] H. Poincaré: *Les méthodes nouvelles de la Mécanique Céleste*, Gauthier-Villars, Paris (1892), reprinted by Blanchard (1987).
- [42] H. Poincaré: *Leçons de Mécanique Céleste*, tomes I–II, Gauthier-Villars, Paris (1905).
- [43] J. Pöschel: *On elliptic lower dimensional tori in Hamiltonian systems*, *Math. Z.*, **202**, 559–608 (1989).
- [44] J. Pöschel: *A KAM-theorem for some nonlinear PDEs*, *Ann. Scuola Norm. Pisa Cl. Sci.*, **23**, 119–148 (1996).
- [45] P. Robutel: *Stability of the Planetary Three-Body Problem — II. KAM Theory and Existence of Quasiperiodic Motions*, *Celestial Mechanics and Dynamical Astronomy*, **62**, 219–261 (1995).
- [46] M. Sansottera, U. Locatelli and A. Giorgilli: *On the stability of the secular evolution of the planar Sun–Jupiter–Saturn–Uranus system*, *Math. Comput. Simul.*, doi:10.1016/j.matcom.2010.11.018 (2011).

- [47] E.M. Standish: *JPL Planetary and Lunar Ephemerides, DE405/LE405*, Jet Propulsion Laboratory — Interoffice memorandum, **IOM 312.F – 98 – 048** (1998).